Supplemental Methods:

Intestinal tissue samples of IBD patients. Tissue specimens were obtained from areas of active disease from the ileum, the sigmoid, the rectum, the colon ascendens and the colon transversum of UC and CD patients. A pathologist blinded to all clinical and endoscopic data of the respective patient performed histological assessment of inflammatory activity in the respective segments. For grading the biopsies as mild [score 1], moderate [score 2] or severe [score 3], the pathologist used morphological features according to the Robarts and Nancy classifications for ulcerative colitis (1-3) and the grading system according to Knieling et al. for Crohn`s disease (3). Lesions without pathological findings were graded as 0. Immunohistochemical stainings were not performed and are not part of the routine diagnostics for activity grading in IBD. mRNA was extracted and Arg1 expression within that lesions was assessed.

Antibiotic treatment and fecal microbiota transfer (FMT). *Arg1*-deficient and *Arg1*-expressing littermate recipients were treated with ampicillin (A; 1 g/L; Roth), vancomycin (V; 500 mg/L; Roth), neomycin sulfate (N; 1 g/L; Pharmacia/Upjohn), streptomycin (2 mg/mL; Sigma) and metronidazole (M; 1 g/L; Sigma) in drinking water for 7 days to remove indigenous gut microorganisms. Three days later 200 mg of fresh stool was collected from respective donor mice immediately upon defecation, resuspended in 5 ml PBS, vortexed for 3 minutes and allowed to settle by gravity for 2 minutes. Transfer into recipient mice was achieved by gavage with 200 µL of the supernatant from the fecal sample every day for one week. Fresh stool was collected every day. One day after the last reconstitution DSS was applied as described in methods.

Histology and H&E staining. Intestinal tissue was fixed in 10% buffered formalin, embedded in paraffin, and cut into 2-µm-thick sections. Colonic and ileal sections were deparaffinized, stained with hematoxylin and eosin by the Department of Pathology and the

Medical Department I of the Friedrich-Alexander Universität Erlangen-Nürnberg, and evaluated microscopically in a double-blinded manner. Briefly, the intestinal damage shown in the presented figures was evaluated using the following four parameters: (i) inflammatory infiltrate in the lamina propia, (ii) thickness of the subepithelial collagenous layer, (iii) presence of intraepithelial lymphocytes, and (iv) epithelial damage. A histologic grading of the severity of the tissue damage was performed for each parameter (score between 0 and 3), leading to a cumulative score between 0 (no signs of inflammation) and 12 (very severe inflammation and epithelial damage).

Immunohistochemistry. Frozen, TissueTek®-embedded intestinal tissue sections (4 µm) were cut with a microtome cryostat (CyroStar NX70, Thermo Scientific), thawed onto adhesion slides (superfrostTM ultra plus, Thermo Scientific), air-dried, fixed with cold acetone (-20 °C) for 10 minutes, air-dried again and surrounded with PAP PEN® (Science Services). The samples were rehydrated for 15 minutes with PBS/0.01% Tween 20 and non-specific binding sites were blocked for 30 minutes with PBS/20% FCS/1% BSA. For Arg1 staining, the sections were blocked with PBS/5% normal donkey serum (Dianova)/0.1% Saponin. Primary antibodies (goat anti-mouse Arg1 [Santa Cruz, clone V-20]; rabbit anti-mouse NOS2 [gift of C. Nathan, New York, clone 3055E]; rat anti-mouse CD31 [Dianova, clone SZ31] and rat anti-mouse CD11b [BD Biosciences, clone M1/70] were diluted in PBS/0.5% BSA or normal donkey serum (Arg1 staining). Tissue sections were incubated overnight at 4°C. After washing with PBS/0.01% Tween 20, fluorochrome-conjugated secondary antibodies (donkey anti-goat [Dionova, clone 114772 and Abberior, clone 10022015CW]; donkey anti-rabbit [Dianova; clone 115275] and goat anti-rat [Invitrogen, clone 714287] were added for 30 minutes each, followed by extensive washing steps. For the detection of NO, unfixed frozen tissue sections were stained with 10 µM 1,2-diaminoanthraquinone (DAQ, Sigma-Aldrich) in PBS, 10% DMSO at 37°C for 45 min, followed by extensive washing steps. Nuclei were stained with DAPI and the sections were finally mounted in Vectashield (Vector labs), covered with a cover slip and dried in the dark for at least 12 hours at 4°C.

Bone marrow chimeras and bone marrow reconstitution. For the preparation of mixed bone marrow radiation chimeras, a mixture of 5 × 10^6 *CD45.2*$^+$ *Tie2-Cre Arg1*$^{fl/fl}$ and 5 × 10^6 *CD45.1*$^+$ B6 bone marrow cells was injected intravenously into 7-12-weeks-old *CD45.2*$^+$ *Tie2-Cre Arg1*$^{fl/fl}$ recipients that had been irradiated twice within a 4-hour interval (first dose 500 rad, second dose 400 rad; Gamma Cell 2000, Molsgaard Dental A/S, Copenhagen, Denmark) one day prior to the transfer. For the reconstitution of bone marrow in irradiated constitutive *Cdh5-Cre Arg1*$^{fl/fl}$ and *Arg1*$^{fl/fl}$ mice, either 5 × 10^6 *Cx3cr1-Cre Arg1*$^{fl/fl}$ or 5 × 10^6 *Arg1*$^{fl/fl}$ bone marrow cells were injected intravenously into 7-12-weeks-old recipients that had been irradiated twice within a 4-hour interval (first dose 500 rad, second dose 400 rad; Gamma Cell 2000, Molsgaard Dental A/S, Copenhagen, Denmark) one day prior to the transfer. The reconstitution of the mixed bone marrow chimeras was determined 6 to 8 weeks after bone marrow injection by FACS analysis.

Determination of vessel density. Formalin-fixed paraffin-embedded intestinal tissue sections (4 µm) were deparaffinized in xylol (Merck Chemicals, Darmstadt, Germany) and rehydrated in descending ethanol series. After antigen retrieval in a target retrieval solution (pH 9.0; TRS9; Dako), slides were treated with 7.5% hydrogen peroxide for 10 minutes at room temperature to block endogenous peroxidases. Endogenous biotin was blocked with the Vector biotin blocking kit (Vector Laboratories). Sections were incubated with a monoclonal rat anti-mouse CD31 antibody (clone SZ31; Dianova) for 1 hour at room temperature. Subsequently, sections were incubated for 30 minutes with a mouse absorbed biotinylated rabbit anti-rat IgG antibody. For CD31 immunofluorescence, an additional protein block (Dako) was performed before incubation with the primary antibody. Slides were incubated overnight at 4°C and further processed using the TSA Cyanine 3 System (Perkin Elmer, Shelton, CT). Nuclei were stained with DAPI, and slides were mounted with fluorescence mounting medium (Dako). Microvessel density was quantified in three optical fields with a magnification of 20x after the identification of vascular hot spots with continuous CD31 expression and obvious lumens for each tissue section. The intensity of the staining was scored as 0, 1, 2, or 3 indicating absence of staining

or weak, moderate, or strong staining intensity, respectively. Based on these scores average vessel densities and standard deviations were calculated.

***Microbiome analyses*.** Fecal specimens were analyzed for the composition of the intestinal microbiome by 16S rRNA gene sequencing. Bacterial genomic DNA from stools was isolated using a ZR Fecal DNA MicroPrepTM kit (Zymo research, Irvine, USA). The V3+4 region of the 16S rRNA gene was amplified using 10 ng of bacterial template DNA with degenerate region-specific primers containing barcodes and Illumina flow cell adaptor sequences (4) in a reaction consisting of 25 PCR cycles (98°C 15 sec, 58° C 20 sec, 72° C 40 sec) using the NEBNext Ultra II Q5 Master Mix (New England Biolabs). Amplicons were purified with Agencourt AMPure XP Beads (Beckmann Coulter), normalized and pooled before sequencing on an Illumina miseq device using a 600-cycle paired-end kit and the standard Illumina HP10 and HP11 sequencing primers. Subsequently, the read fastq files were bioinformatically processed (merging, demultiplexing, quality filtering, dereplication, chimera removal) using the 64 bit version of Usearch 10 according to the Uparse pipeline (5). Operational taxonomic units (OTUs) were picked at a threshold of 97 % similarity and taxonomically classified by comparing the representative OTU sequence to the reference file of the ribosomal database project (RDP version 16). Alpha diversities, samples distances and relative differential abundances after rarifying were calculated with MicrobiomeAnalyst (6). P-values of <0.05 and LDA score ≥ 2.0 were considered significant in Kruskal-Wallis and pairwise Wilcoxon tests, respectively. P-values were FDR-corrected.

Two photon microscopy and three dimensional reconstruction. Confocal imaging was performed by 2-photon microscopy on a Zeiss LSM 880 NLO equipped with a 680-1300 nm tunable & fixed 1040 nm 2-photon laser from Newport SpectraPhysics. Two-photon images were acquired with a 20x W-Plan Apochromat objective lens. Alexa Fluor 594 was excited at 780 nm and specific emission was detected at 575-610 nm. Additionally, the second harmonic generation (SHG) signal was acquired using the fixed 1040 nm laser line and detected at 500-

500 nm. For both channels non-descanned GaAsP detectors were used. Reconstruction of the volumes was performed with 3Dscript (7).

Cell purification. Intestines of mice were removed, cleaned from feces and Peyer`s patches and cut into small pieces. The intestinal pieces were transferred into a conical flask containing pre-warmed 1mM EDTA PBS. The minced intestinal segments were added to pre-warmed 2%(vol/vol) FBS RPMI before digestion with 20µg/mL liberase DH and 50µg/mL DNase I. These mixtures were repeatedly passed through an 18-gauge needle. ILC2s were enriched from the obtained suspensions with the EasyStep mouse ILC2 enrichment kit following manufacturer`s instructions (Stemcell, Vancouver, Canada). Obtained cells were stained with propidium iodide (PI) and an antibody cocktail containing CD3e (clone 145-2C11), CD11b (clone M1/70), CD11c (clone N418), CD45 (clone 30-F11), Ter119 (clone TER-119), γ/δ TCR (clone GL-3), CD19 (clone 1D3), NK1.1 (clone PK136) and Gr-1 (clone RB6-8C5). After the selection of live cells with PI, $CD45^{+}Lin^{-}$ cells were gated and subsequently purified on a FACS Aria II (BD Biosciences, Franklin Lakes, NJ, USA) (purity of > 95%). The identity of ILC2s was confirmed by surface/intracellular staining for KLRG1, Sca-1 and GATA-3 (see table for flow antibodies below) and subsequent FACS analysis.

Intestinal epithelial cells were separated from the underlying tissue by incubation in 30 mM EDTA in Ca^{2+}- and Mg^{2+}-free PBS for 10 minutes at 37°C followed by vigorous shaking as described (8). Cells were harvested by centrifugation, washed, and multicellular epithelial aggregates were purified by repeated differential sedimentation at 1*g* in ice-cold PBS from contaminating cells and residual tissue.

qPCR. Total RNA was extracted from homogenized tissue or cultured cells using the TRIfast reagent (Peqlab). Then, 1 µg RNA were reverse transcribed using the High-Capacity cDNA Archive Kit (Thermo Fisher Scientific). Next, qPCR was performed on the ABI7900HT Fast Real Time PCR system (Applied Biosystems; Thermo Fisher Scientific). For the detection of *Arg1* (Mm01190441_g1), *Arg2* (Mm00477592_m1), *Nos2* (Mm00440485_m1), *Tnf* (Mm00443258_m1), *Il17a* (Mm00439618_m1), *Il18* (Mm00434226_m1), *Myd88*

(Mm00440338_m1), *Cdh11* (Mm00515466_m1), *Cdh24* (Mm01313848_g1), *Pcdh12* (Mm00450488_m1), *Pcdh16* (Mm01165391_m1), *Pcdh18* (Mm00499890_m1), *Pcdh19* (Mm01340474_m1), *Ctnna3* (Mm00617137_m1), *Ctnnb1* (Mm00483039_m1), *Trcpc3* (Mm00444690_m1), *Chk2* (Mm00443839_m1), *Odc* (Mm02019269_g1), *Tlr2* (Mm00442346_m1), *Tlr4* (Mm00445273_m1), *Md2* (Mm01227593_m1), *Cd14* (Mm00438094_g1), *Tlr5* (Mm01312198_s1), *Tlr8* (Mm01157262_m1), *Tlr9* (Mm00446193_m1), *Tlr11* (Mm01701924_s1), *Lbp* (Mm00493139_m1), *Ifngr1* (Mm00599890_m1), *Il1r2* (Mm00439629_m1), *Il4Ra* (Mm01275139_m1), *Il22* (Mm00444241_m1), *Il33* (Mm00505403_m1), *Hif1a* (Mm00468875_m1), *Il13* (Mm00434204_m1), *Il12rb2* (Mm00434200_m1), *Il6ra* (Mm00439653_m1), *Il23r* (Mm00519943_m1), *Il1b* (Mm00434228_m1), *Sms* (Mm00786246_s1), *Srm* (Mm00726089_s1), *Slc7a2* (Mm00432032_m1), *Adometdc* (Mm04207265_gH), *Smox* (Mm01275475_m1), *Agat* (Mm00491879_m1), *Agmat* (Mm01348862_m1), *Asl* (Mm01197741_m1), *Ass* (Mm00711256_m1) and *Hprt* (Mm00446968_m1) gene-specific assays with FAM as probe from Life Systems (Mönchengladbach, Germany) were used. *Ifng* (forward: 5`-atctggaggaactggcaaaa-3`; reverse: 5´-ttcaagacttcaaagag tctgaggta-3`), *Il10* (forward: 5`-cagagccacatgctcctaga-3´; reverse: 5`-gtccagctggtcctttgttt-3´) and *Hprt* (forward: 5`-tcctcctcagaccgctttt-3´; forward: 5`-cctggttcatcatcgctaatc-3´) were detected using the Roche system (Basel, Switzerland). Human *Arg1* was assayed using probe Hs00968979_m1 from Thermofisher. The mRNA levels were calculated using the following formula: relative expression = $2^{-(C_{T(Target)} - C_{T(Endogenous\ control)})} \times f$, with $f = 10^4$ as an arbitrary factor. Relative expression was calibrated to controls, as indicated in the legends.

Cell preparation and culture. Bone marrow-derived mouse macrophages or DCs were collected after 7 days of culture in DMEM or RPMI 1640 medium supplemented with glutamine, antibiotics, and 10% FCS with 2 ng/mL mouse M-CSF (macrophages) and 2 ng/mL GM-CSF (DCs) (all from R&D Systems, Minneapolis, MN). Where indicated, cells were stimulated with 100ng/mL LPS or *E. coli* at an MOI of 10 under norm- and hypoxic conditions (pO_2 20% or pO_2 1%, respectively) in RPMI for 24 or 48 hours, respectively.

1×10^5 $CD45^+$ hematopoetic cells/well isolated from the colons of DSS-treated mice were stimulated with a mixture of ligands for TLR2 (10^8 HKLM /mL), TLR4 (100ng LPS /mL), TLR5 (500ng FLA-ST/mL) and TLR9 (50µM ODN1826) or plate bound anti-CD3 (100ng/mL) for 72 hours. Cytokines in the cell culture supernatants were measured using the respective DuoSet ELISAs from R&D Systems (Minneapolis, MN, USA) or MBL (Woburn, MA, USA) following the manufacturer's instructions.

Cell harvesting, analyte extraction from the pellets and spiking experiment. For amino acid analysis, stool specimens were weighed (4.1 mg – 14.2 mg) and extracted with 600µL 80% methanol. Prior to extraction, 10 µL of an internal standard containing ^{13}C, ^{15}N labeled amino acids (100 µM each) were added to the sample. The samples were vortexed, sonicated, and centrifuged (9560xg, 5min, 4 °C). The supernatant was collected and the extraction step was repeated twice with 200µL 80% methanol and the last wash was centrifuged at 13800xg. All supernatants were combined, dried in a vacuum evaporator (CombiDancer, Hettich AG, Bach, Switzerland) and the residue was then re-dissolved with 100µL water. A 10µL aliquot of the final sample extract was subjected to propyl chloroformate/propanol derivatization and subsequent analysis by HPLC-ESI-MS/MS as previously described (9).

Creatine and creatinine were analyzed in a separate stool aliquot using the same extraction protocol but with creatinine-d3 as internal standard. Sample extracts were analyzed by HPLC-ESI-MS/MS with positive mode ionization and multiple reaction monitoring (MRM) employing an API 4000 QTrap mass spectrometer (ABSciex, Darmstadt, Germany) and a 1200 SL HPLC system (Agilent, Boeblingen, Germany). Separation was performed on an Atlantis T3 (2.1 × 150 mm, 3 µm, Waters, Eschborn, Germany) with a Security Guard column (C18, Phenomenex, Aschaffenburg, Germany) using gradient elution with 0.1% formic acid in water (v/v) as mobile phase A and 0.1% formic acid in acetonitrile (v/v) as mobile phase B. An injection volume of 5 µL was employed. Quantification was performed using calibration curves with creatinine-d3 as internal standard.

For the determination of L-arginine and polyamines in serum and stool respective samples were repeatedly dried under nitrogen flow and wetted with derivatization buffer, consisting of equal parts of pyridine, ethanol and water as described (10). Derivatization was performed using 5% phenyl isothiocyanate (PITC) for 30 minutes at room temperature. Samples were dried again and dissolved in methanol containing 5mM ammonium acetate. Separation and quantitation of the resulting phenylthiocarbamyl derivatives was accomplished by reverse-phase liquid chromatography coupled to an ESI-MS/MS-system with positive ionization mode (API6500+, Sciex Darmstadt, Germany, HPLC1260 series, Agilent Technologies, Waldbronn, Germany). For the liquid chromatography part an Agilent Eclipse XDB-C18 (3.5µm, 3x100 mm) column was used as stationary phase. Mobile Phase was made up out of two solutions: 0.2% formic acid in water and 0.2% formic acid in acetonitrile running a gradient ramping towards higher acetonitrile content. The following transitions including the matching deuterated internal standards for quantitation were used for measurement in MRM-mode: arginine *m/z* 310.1/217.0, arginine-d_7 *m/z* 317.1/224.0, agmatine *m/z* 266.1/173.1 (*m/z* 266.1/207.1), agmatine-d_8 *m/z* 274.2/181.2, putrescine *m/z* 266.1/113.9, putrescine d_8 *m/z* 367.2/274.2, spermidine *m/z* 551.2/193.2, spermidine –d_6 *m/z* 557.2/199.2, spermine *m/z* 608.3/193.2 (*m/z* 473.3/193.2), spermine-d_{20} *m/z* 628.3/199.2 (*m/z* 493.6/199.2).

Western blot analysis. Cell cultures were washed three times with warm PBS and lysed by sonication using a Branson Sonifier B-12 in 40 mM Tris buffer (pH 8.0) containing 1mM PMSF and a protease inhibitor mix (complete mini EDTA-free, Roche), followed by quantification of the protein content of the supernatants using the DC Protein Assay (Bio-Rad). Cell lysates were separated by 10% SDS-PAGE (loading of 40-80 µg protein/lane) and transferred to a PVDF membrane (0.45 µm, Millipore Immobilon-P, 1 hour, constant current of 1 A) using the tank blot technique. To block non-specific binding sites, the blotted membranes were placed in 5% nonfat dry milk/0.1% Tween 20 in PBS for at least 1 hour. For detection of the target proteins, blots were analyzed by ECL-based chemiluminescence (ECL Plus Pierce® Western Blotting Substrate) using primary and secondary antibodies (see table below). If necessary,

blots were stripped (RestoreTM Western Blot Stripping Buffer, Thermo Scientific) and reprobed. Protein expression was visualized on an Intas ChemiLux Imager and images were processed with help of the Adobe Photoshop CS5-software (Adobe Systems, San José, CA, USA). The fluorescence intensity of the proteins of interest was quantitated by ImageJ software.

Table: Antibodies used for Western blot

Antibody	Source, Reference	Catalog No.	Batch, Clone
goat anti-arginase 1	Santa Cruz Biotechnology	sc-18354	V-20
rabbit anti-actin	Sigma Aldrich	A2066	polyclonal
rabbit anti-HSP90	Santa Cruz Biotechnology	7947	H114
rabbit anti-mouse NOS2	gift of C. Nathan, New York	n.a.	3055E
donkey anti-goat	Dianova	705035147	54065
goat anti-mouse	Dianova	115035166	55890
goat anti-rabbit	Dianova	111035144	78268

Flow cytometry and intracellular cytokine staining. Antibodies against mouse CD11b, F4/80, Gr1, CD11c, CCR2, CCR5, $\alpha 4\beta 7$, LFA-1, CD103, C5aR, E-cadherin, EpCam, TCRβ, CD4, CD8, γ/δ TCR,B220, CD45.1, CD45.2, CD3e, CD5, CD45R, Ly-6B.2, Ter119, Siglec-F, NK1.1, KLRG1, Sca-1 and GATA-3 were purchased from eBioscience, R&D Systems, BD and AbD serotec (see table below). Cells were analyzed on a BD FACS Canto II (BD Biosciences, San Diego, CA) with FlowJo software (Tree Star).

Table: Antibodies used for FACS analysis

Antibody	Source, Reference	Catalog No.	Batch, Clone
CD11b	eBioscience	25-0112-82 11-0112-82 17-0112-83 12-0112-82	M1/70
F4/80	eBioscience	45-4801-82 17-4801-82	BM8
Gr1	eBioscience	45-5931-80 17-5931-82 12-5931-82	RB6-8C5
CD11c	eBioscience	11-0114-85 45-0114-82 17-0114-82 12-0114-83 47-0114-82	N418
CCR2	R&D Systems	FAB5538P	475301
CCR5	eBioscience	17-1956-42	NP-6G4
$\alpha 4\beta 7$	eBioscience	17-5887-80	DATK32
LFA-1	eBioscience	46-0111-80	M17/4
CD103	eBioscience	11-1031-85	2E7
C5aR	AbD Serotec	MCA2457PE	20/70
E-cadherin	eBioscience	46-3249-80	DECMA-1
EpCam	eBioscience	E50-2440	G8.8
TCRβ	eBioscience	11-5961-82 E50-2440 48-5961-82	H57-597
CD4	eBioscience	11-0041-86 17-0041-82 12-0041-82 48-0042-80A	GK1.5 RM4-5
CD8	eBioscience	11-0081-85 45-0081-80 17-0081-82 12-0081-82	53-6.7
γ/δ TCR	eBioscience	17-5711-82 12-5711-82 46-5711-82	GL-3
B220	eBioscience	11-0452-82 12-0452-82 25-0452-82	RA3-6B2

CD45.1	eBioscience	11-0453-85 17-0453-82	A20
CD45.2	eBioscience	11-0454-85 45-0454-80	104
CD3e	eBioscience	17-0032-82 45-0031-82	17A2 145-2C11
CD5	eBioscience	17-0051-82	52-7.3
CD45RB	eBioscience	11-0455-82	30-F11
Siglec-F	BD	562680	E50-2440
NK1.1	eBioscience	25-5941-81 17-5941-82	PK136
KLRG1	eBioscience	17-5893-82	2F1
Sca-1	eBioscience	17-5981-82	D7
GATA-3	eBioscience	46-9966-41	TWAJ

Transwell permeability assay. $4x10^5$ endothelial cells (mLEND) (11) were seeded in polycarbonated Nunc™ cell culture inserts (pore size 8µm) in 6-well plates (Thermo scientific, Dreieich, Germany) and grown to confluence for 48 hours. Membranes without mLEND monolayers were used as controls. $5x10^5$ bone marrow derived macrophages from wild type mice were added to cell culture media containing 1% FCS in the upper wells and respective L-arginine concentrations of 0%, 1% and 3%. The medium in the lower compartment was supplemented with 10ng/mL MCP-1. Two days later non-migratory cells on top of the membranes as well as the transmigrated cells on the bottom of the wells were harvested, stained with CD45, CD11b and F4/80 and counted using flow cytometry. The numbers of the permeated cells were displayed in the respective figures.

Supplemental Figures:

Supplemental Figure 1. Hypoxia, inflammation and bacteria upregulate Arg1 in myeloid and endothelial cells. (**A**-**C**) The expression of *Arg1* was assessed by qPCR (**A** and **B**) and Western blot analysis (**C**) in purified ILC2s (**A**), colon tissue, lamina propria (LP), intestinal epithelium (IE) (**B**) and the endothelial cell line mlEND (11) (**C**). ILC2s (**A**), colon tissue, LP and IE (**B**) were purified from the gut of 3-8 individual, DSS-treated and untreated 10 weeks old female B6 mice each. The ratio of the *Arg1* copies relative to the *Hprt* copies was calculated. (**A** and **B**) The relative increase in *Arg1* copy numbers comparing naïve and DSS-treated mice is displayed. Data were analyzed using student's t-test or the Mann-Whitney test (*, p≤0.05; **, p<0.01). Error bars indicate the SD of the mean. (**C**) Endothelial cells were cultured for 48 hours under normoxic (pO_2 20%) and hypoxic conditions (pO_2 1%) and stimulated with *E. coli* at a MOI of 10.

Supplemental Figure 2. The induction of *Arg1* expression by oxazolone depends on the intestinal microbiota and IL-4/IL-13. (**A**-**C**) Using qPCR the expression of *Arg1* was assessed before (**A**) and after (**A** and **B**) oxazolone application, with or without application of broad-spectrum antibiotics (AB) (**B**) in total colonic tissue of pathogen-free (SPF) B6 mice (**A** and **B**) or of *Il4*/ *Il13*$^{-/-}$ mice and respective wild-type littermate controls (*Il4*/ *Il13*$^{+/+}$) (**C**). The ratio of *Arg1* mRNA copies relative to *Hprt* copies was calculated in the indicated tissues of 4-12 individual female mice. The relative increase in *Arg1* copy numbers of naive versus DSS-treated mice is displayed. Data were analyzed using the Mann-Whitney test (*, p≤0.05; **, p<0.01). Error bars indicate the SD of the mean.

Supplemental Figure 3. The deletion of *Arg1* in either epithelial cells, myeloid cells, endothelial cells, or in ILC2s is not sufficient to significantly alter the severity of colitis. (**A** and **B**) The severity of colitis (**A**) and wasting disease (**B**) in 16 *Villin-Cre Arg1*$^{fl/fl}$ mice and 11 *Arg1*-expressing littermate controls (*Arg1*$^{fl/fl}$) each was monitored by high-resolution endoscopy and weight recording. The means (± SD) of the endoscopic scores are displayed

(**A**). The change of body weight was represented as percentage difference from the initiation day of the study (**B**). (**C** and **D**) Using qPCR the expression of *Arg1* was assessed in myeloid cells purified from the lamina propria of *Villin-Cre Arg1*$^{fl/fl}$ mice (**C**) and in intestinal epithelial cells (IEC) purified from *Tie2-Cre Arg1*$^{fl/fl}$ mice (**D**). The ratio of *Arg1* mRNA copies relative to *Hprt* copies was calculated in the indicated cells of 3-10 individual female mice. The relative increase in *Arg1* copy numbers of DSS-treated knockout and wild-type mice (*Arg1*$^{fl/fl}$) is displayed. (**E**-**H**) The severity of colitis in the indicated conditional *Arg1* knockout strains, respective wild-type littermate controls (*Arg1*$^{fl/fl}$) (**E**-**G**) and bone marrow chimeras (**H**) was monitored by high-resolution endoscopy. The means (± SD) of the endoscopic scores from 4 (**E**), 6 (**F**) and 9 (**G**) individual knockout female mice and 4-7 respective littermate controls as well as 9-12 *Arg1*$^{fl/fl}$/*Arg1*$^{fl/fl}$, *Cx3cr1-Cre Arg1*$^{fl/fl}$/*Arg1*$^{fl/fl}$, *Arg1*$^{fl/fl}$/*Cdh5-Cre Arg1*$^{fl/fl}$ and *Cx3cr1-Cre Arg1*$^{fl/fl}$/ *Cdh5-Cre Arg1*$^{fl/fl}$ bone marrow chimeras (**H**) are displayed. Depending on the number of groups and the distribution of data, data were analyzed using one way ANOVA followed by a Bonferroni post-hoc test for pairwise comparisons if the former was significant, the Mann-Whitney test or the Kruscal-Wallis test followed with Dunn´s multiple comparisons if the former was significant (*, p≤0.05; **, p<0.01; ***, p<0.001). Error bars indicate the SD of the mean.

Supplemental Figure 4. *Tie2-Cre Arg1*$^{fl/fl}$ mice loose weight to a similar degree as Arg-expressing litters (*Arg1*$^{fl/fl}$). (**A**-**C**) Relative changes in body weight were monitored in *Tie2-Cre Arg1*$^{fl/fl}$ mice and respective littermate controls (*Arg1*$^{fl/fl}$ over one (A, B) or three cycles of DSS (C) in 5 female (**A** and **C**) and male mice (**B**), respectively. Mice were treated with three cycles of DSS in their drinking water for 7 days, followed by 14 days of regular water for the first two cycles and by 3 days of regular water after the last cycle.

Supplemental Figure 5. The deletion of *Arg1* within the endothelial and hematopoietic cell compartment ameliorates oxazolone-induced colitis. (**A**) Wasting disease in 10 *Tie2-Cre Arg1*$^{fl/fl}$ mice and 9 littermate controls (*Arg1*$^{fl/fl}$) was monitored by survival. For comparison

Kaplan–Meier survival curves were plotted for each mouse strain, and statistical significance was determined by log rank test (*, p≤0.05). (**B**) The severity of colitis in surviving *Tie2-Cre Arg1*$^{fl/fl}$ mice and respective littermate controls (*Arg1*$^{fl/fl}$) was monitored by histopathological analyses of H&E-stained tissue sections on day 4. The means (± SD) of the histological scores are displayed. Data were analyzed using the Mann-Whitney test (**, p<0.01). Error bars indicate the SD of the mean.

Supplemental Figure 6. The deletion of *Arg1* within the endothelial and hematopoietic cell compartment ameliorates T cell transfer colitis. (**A**-**D**) The induction of intestinal inflammation in *Rag1*$^{-/-}$ recipients upon transfer of naive CD4$^+$ T cells from *Tie2-Cre Arg1*$^{fl/fl}$ and wild-type litters (*Arg1*$^{fl/fl}$) (**A** and **B**) as well as in *Rag1*$^{-/-}$ *x Arg1*$^{fl/fl}$ and *Rag1*$^{-/-}$ *x Tie2-Cre Arg1*$^{fl/fl}$ recipients upon transfer of T cells from wild-type donors (*Arg1*$^{fl/fl}$) (**C** and **D**) was monitored by high-resolution endoscopy (**A** and **C**) and histopathological analysis of hematoxylin and eosin (H&E)-stained tissue sections (**B** and **D**). The means (± SD) of the endoscopic and histological scores from 3-5 individual recipient mice 4.5 weeks after T cells transfer are displayed. Data were analyzed using the Mann-Whitney test ((*, p≤0.05; **p<0.01).

Supplemental Figure 7. Arg1 enhances myeloid cell adhesion. (**A**-**K**) The distribution of myeloid cells harvested from the lamina propria (**A**-**G**) and from the blood that drains intestinal tissues (**H**-**K**) of *Tie2-Cre*$^{+/-}$*Arg1*$^{fl/fl}$ mice and respective littermate controls (**A**-**C** and **H**-**K**) as well as of *Ly5.1*$^+$/*Ly5.1*$^-$ wild-type (*Arg1*$^{fl/fl}$)/*Tie2-Cre Arg1*$^{fl/fl}$ bone marrow chimeric mice (**D**-**G**) was assessed by flow cytometry. Representative FACS plots reflecting the gating strategies for the indicated cell populations (**A**-**I**) along with their CCR2 (**J**) and C5aR (**K**) expression are displayed. Gate 1 (**F**) reflects the distribution of Gr1$^+$ CD11b$^+$ cells within the *Arg1*-expressing compartment in chimeric mice while gate 2 (**G**) represents the same subset with *Arg1*-deficient cells.

Supplemental Figure 8. Major pathways of arginine metabolism. ADC, arginine decarboxylase; AdoMetDC, S-adenosylmethionine decarboxylase; AGAT, arginine:glycine amidino transferase; AGMAT, agmatinase; Arg, arginase; ASL, argininosuccinate lyase; ASS1, argininosuccinate synthase 1; GAMT, guanidinoacetate N-methyl-transferase; NOS, nitric oxide synthase; OAT, ornithine aminotransferase; ODC, ornithine decarboxylase; OTC, Ornithine transcarbamylase; SMS, spermine synthase; SMOX, spermine oxidase; SRM, spermidine synthase.

Supplemental Figure 9. Deletion of *Arg1* does not affect the mRNA expression of major arginine-metabolizing enzymes. (**A**-**E**) The expression of the ornithine transcarbamylase (*Otc*) (**A**), argininosuccinate synthase (*Ass*) (**B**), argininosuccinate lyase (*Asl*) (**C**), arginine:glycine amidino transferase (*Agat*) (**D**) and guanidinoacetate methyltransferase (*Gamt*) (**E**) was determined in colon tissues of DSS-treated *Tie2-Cre Arg1*$^{fl/fl}$ mice and *Arg1*-expressing littermate controls (*Arg1*$^{fl/fl}$) by RNAseq. (n=3-4). **(F)** The concentration of creatine was determined by HPLC in the feces. (**G**-**I**) The expression of agmatinase (*Agmat*) (**G**) and ornithine aminotransferase (*Oat*) (**H**) and the concentration of proline (**I**) were determined by RNAseq in colonic tissues and by HPLC in the feces. (n=3-5). (**J**) The severity of colitis in *Tie2-Cre Arg1*$^{fl/fl}$ mice with and without treatment with the NOS2 inhibitor N^6-(1-iminoethyl)-L-lysine (L-NIL) was monitored by endoscopy. The means (± SD) of the endoscopic scores from 8 individual knockout female mice each are displayed. Data were analyzed using the Mann-Whitney test (*, $p \leq 0.05$; ***, $p < 0.001$).

Supplemental Figure 10. The consumption of L-arginine enhances DSS-induced colitis. (**A**) The expression of *Arg1*, *Nos2* and *Il17* was determined by qPCR in colon tissues of individual DSS-treated *Tie2-Cre Arg1*$^{fl/fl}$ mice fed control or arginine-free chow, respectively. The ratio of the mRNA copies of the indicated genes relative to the *Hprt* copies was calculated. The relative increase in the respective gene copy numbers comparing mice fed with control chow or arginine-free chow is displayed. (**B** and **C**) The severity of wasting disease (**B**) and

colitis (**C**) in naïve and DSS-treated *Tie2-Cre Arg1*$^{fl/fl}$ mice fed control or arginine-free chow was monitored by weight recoding (**B**) and high-resolution endoscopy (**C**). The change of body weight was represented as percentage difference from the initiation day of the study (**B**). Representative endoscopy pictures are displayed (**C**). Depending on the number of groups and the distribution of data, data were analyzed using the Mann-Whitney test or the Kruscal-Wallis test followed with Dunn´s multiple comparisons if the former was significant (*, p≤0.05; **, p<0.01). (n=4-10). Error bars indicate the SD of the mean.

Supplemental Figure 11. Nutritional restriction of L-arginine enhances oxazolone-induced colitis. (**A** and **B**) Wasting disease (**A**) and the severity of colitis (**B**) in oxazolone-treated wild-type littermates fed arginine-supplemented (n=6) or arginine-deficient chow (n=10) was monitored by survival rates (**A**) and by histopathological analyses of H&E-stained tissue sections on day 4 (**B**). For comparisons of survival, Kaplan–Meier survival curves were plotted for each group (**A**), and statistical significance was determined by log rank test (**, p<0.01). The means (± SD) of the histological scores from the surviving mice are displayed (**B**). Data were analyzed using the Mann-Whitney test (*, p≤0.05). Error bars indicate the SD of the mean.

Supplemental Figure 12. The accumulation of polyamines and the expression of *Odc* are reduced in DCs from *Tie2-Cre Arg1*$^{fl/fl}$ mice. (**A** and **B**) The expression of the ornithine decarboxylase (*Odc*) (**A**) and the accumulation of polyamines (**B**) were assessed by qPCR and HPLC in bone marrow derived DCs from *Tie2-Cre Arg1*$^{fl/fl}$ and *Arg1*-expressing littermates (*Arg1*$^{fl/fl}$) before and after stimulation with *E. coli in vitro* (n=3-4). Data were analyzed using one-way ANOVA followed by a Bonferroni post-hoc test for pairwise comparisons if the former was significant (*, p≤0.05; ***, p<0.001). Error bars indicate the SD of the mean.

Supplemental Figure 13. Deletion of *Arg1* does not affect polyamine synthesis and degradation in the inflamed colon tissues. (**A**-**D**) The expression of the spermine synthase (*Sms*) (**A**), the spermidine synthase (*Srm*) (**B**), the S-adenosylmethionine decarboxylase

(*Adometdc*) (**C**) and the spermine oxidase *Smox* (**D**) was determined in colon tissues of DSS-treated *Tie2-Cre Arg1*$^{fl/fl}$ mice and *Arg1*-expressing littermate controls (*Arg1*$^{fl/fl}$) by RNAseq. (n=3-4). Error bars indicate the SD of the mean.

Supplemental Figure 14. *Tie2-Cre Arg1*$^{fl/fl}$ mice exhibit an enhanced expression of polyamine target genes in the gut. (**A**-**F**) The expression of catenin alpha 3 (**A**), catenin beta 1 (*Ctnnb1*) (**B**), protocadherin 18 (*Pcdh18*) (**C**), protocadherin 12 (*Pcdh12*) (**D**), cadherin 24 (*Cdh24*) (**E**), protocadherin 16 (*Pcdh16*) (**F**) and protocadherin 19 (*Pcdh19*) (**G**) was determined in colonic tissues of DSS-treated *Tie2-Cre Arg1*$^{fl/fl}$ mice and *Arg1*-expressing littermate controls (*Arg1*$^{fl/fl}$) by RNAseq. Data were analyzed using the Mann-Whitney test (*, p≤0.05; ***, p<0.001). (n=3-4). Error bars indicate the SD of the mean.

Supplemental Figure 15. *Enterobacteriaceae* expand in the feces of *Arg1*-expressing mice. (**A** and **B**) The expansion of *Escherichia spp*. was assessed by 16S rRNA analysis (**A**) and conventional CFU plating assays (**B**) in naïve and DSS-treated *Tie2-Cre Arg1*$^{fl/fl}$ mice and *Arg1*-expressing littermate controls (*Arg1*$^{fl/fl}$). Data for 3-16 individual mice in each group were analyzed using the Mann-Whitney test (*, p≤0.05). Error bars indicate the SD of the mean.

Supplemental Figure 16. *Arg1*-expression of the host enhances intestinal dysbiosis. Feces sampled from the colons of *Tie2-Cre Arg1*$^{fl/fl}$ mice and *Arg1*-expressing littermate controls (*Arg1*$^{fl/fl}$) (n=4) were subjected to 16S rRNA taxonomic analysis before and after DSS application. The composition of the microbiome at the genus level is displayed. The stacked bars show averaged abundancies of the same number of mice. Only taxa with over 1% relative abundance in any sample are shown.

Supplemental Figure 17. The deletion of *Arg1* within endothelial and hematopoietic cells promotes the expansion of an anti-colitogenic microbiota. (**A**-**C**) The composition of the intestinal microbiome was assessed on day 10 by 16S rRNA analysis of fecal samples of 6

Tie2-Cre Arg1$^{fl/fl}$ mice and *Arg1*-expressing littermates (*Arg1*$^{fl/fl}$) (**A** and **B**) as well as from 6 wild-type mice with or without arginine-supplementation (**C**) each. Linear discriminant analyses (LDA) were combined with effect size measurements (LEfSe) and the respective results at the genus level (**A**) as well as principal component analysis (PCA) plots (**B** and **C**) are displayed. The composition of the intestinal microbiota was assessed as depicted in Supplemental Figure 17J on days 0, 7 and 17 before and after L-arginine supplementation and/or DSS application, respectively.

Supplemental Figure 18. The deletion of *Arg1* in endothelial and hematopoietic cells and L-arginine supplementation of wild-type mice promote the expansion of an anti-inflammatory intestinal microbiota. (**A**-**J**) The expansion of *Christensenella* (**A** and **F**), *Ruminococcus* (**B** and **G**), *Fodinicurvata* (**C** and **H**) and *Turicibacter* (**D** and **I**) in *Tie2-Cre Arg1*$^{fl/fl}$ mice and wild-type litters (*Arg1*$^{fl/fl}$) (**A**-**D**) as well as in wild-type mice before and after supplementation with 3%L-arginine (**F**-**I**) are depicted. Error bars indicate the SD of the mean. Stool samples in panels **A**-**D** were analyzed before (day 0) and after (day 10) DSS application as displayed in panel **E**. In addition, stool samples in panels **E**-**H** were evaluated for their microbiota composition also before (day 0) and after (day 7) L-arginine supplementation as depicted in panel **J**.

Supplemental Figure 19. The application of antibiotics prevents wasting disease and ameliorates colitis in DSS-treated B6 recipients. (**A** and **B**) The severity of colitis (**A**) and wasting disease (**B**) upon DSS application in 3 untreated mice and 4 B6 recipients treated with broad-spectrum antibiotics was monitored by high- resolution endoscopy and weight recoding. The change of body weight is represented as difference (%) relative to the start of the experiment /day 0, 100%) (**A**). The means (± SD) of the endoscopic scores for each cohort are displayed (**B**). None of the recipients received a FMT. Data were analyzed using the Mann-Whitney test (*, $p \leq 0.05$**, $p < 0.01$). Error bars indicate the SD of the mean.

Supplemental Figure 20. Recipients of FMTs from *Tie2-Cre Arg1$^{fl/fl}$* donors recover faster from DSS-induced colitis. The severity of colitis in B6 recipients of FMTs from *Tie2-Cre Arg1$^{fl/fl}$* and *Arg1*-expressing (*Arg1$^{fl/fl}$*) donors was monitored by high-resolution endoscopy and histopathological analyses of H&E-stained tissue sections. Representative endoscopy and histopathology pictures for untreated and DSS-treated recipients of feces from *Tie2-Cre Arg1$^{fl/fl}$* and *Arg1*-expressing donors (*Arg1$^{fl/fl}$*) 10 and 15 days after FMT are displayed. Scale bar: 200 µm.

Supplemental Figure 21. Fecal microbiota transplants from *Tie2-Cre Arg1$^{fl/fl}$* donors promote the expansion of an anti-colitic intestinal microbiota in B6 recipients. Feces sampled from the colons of B6 recipients of FMTs from *Tie2-Cre Arg1$^{fl/fl}$* and *Arg1*-expressing donors (*Arg1$^{fl/fl}$*) (n=3) were subjected to 16S rRNA taxonomic analysis before and after DSS application. The stacked bars show averaged abundancies of the same number of mice. Only taxa with over 1% relative abundance in any sample are shown.

Supplemental Figure 22. Fecal microbiota transplants from *Tie2-Cre Arg1$^{fl/fl}$* donors promote the expansion of an anti-colitic intestinal microbiota in B6 recipients. (**A** and **B**) The composition of the intestinal microbiota was assessed by 16S rRNA analysis from the feces of 6 B6 recipients of FMTs from *Tie2-Cre Arg1$^{fl/fl}$* and *Arg1*-expressing donors (*Arg1$^{fl/fl}$*) each on day 10. Linear discriminant analyses (LDA) were combined with effect size measurements (LEfSe) and the respective results at the genus level (**A**) as well as principal component analysis (PCA) plots (**B**) are displayed.

Supplemental Figure 23. The deletion of *Arg1* in FMT recipients neither affects the distribution of myeloid cells nor the expression of cytokines, MyD88 and polyamine target genes. (**A**) The fecal microbiota from naïve *Arg1*-expressing control littermates was transferred into*Tie2-Cre Arg1$^{fl/fl}$* and *Arg1*-expressing control recipients (*Arg1$^{fl/fl}$*) each. The distribution of the indicated cell subsets in each DSS-treated recipient cohort was assessed in

the lamina propria by flow cytometry. (**B** and **C**) The expression of the indicated cytokines (**B**), *Myd88* and polyamine target genes (**C**) was analysed by qPCR in colonic tissues of the respective recipients 10 days after DSS application. The ratio of the mRNA copies of the indicated genes relative to the *Hprt* copies was calculated and the relative increase in the respective gene copy numbers between 8 DSS-treated *Arg1*-deficient and 4 wild-type recipients is displayed. Data were analyzed using the Mann-Whitney test. Error bars indicate the SD of the mean.

Supplemental Video: Arg1 enhances vessel density.

Mice were intravenously injected with anti-CD31 antibodies and the relative blood vessel density in the gut was assessed by two-photon microscopy. Representative videos from naïve (A) or DSS-treated (B, C) *Arg1*-expressing littermate controls (*Arg1*$^{fl/fl}$) (A, B) and *Tie2-Cre Arg1*$^{fl/fl}$ mice (C) are displayed.

Supplemental references

1. Mosli MH, Feagan BG, Zou G, Sandborn WJ, D'Haens G, Khanna R, et al. Development and validation of a histological index for UC. *Gut.* 2017;66(1):50-8.
2. Marchal-Bressenot A, Salleron J, Boulagnon-Rombi C, Bastien C, Cahn V, Cadiot G, et al. Development and validation of the Nancy histological index for UC. *Gut.* 2017;66(1):43-9.
3. Knieling F, Neufert C, Hartmann A, Claussen J, Urich A, Egger C, et al. Multispectral Optoacoustic Tomography for Assessment of Crohn's Disease Activity. *N Engl J Med.* 2017;376(13):1292-4.
4. Fadrosh DW, Ma B, Gajer P, Sengamalay N, Ott S, Brotman RM, et al. An improved dual-indexing approach for multiplexed 16S rRNA gene sequencing on the Illumina MiSeq platform. *Microbiome.* 2014;2(1):6.
5. Edgar RC. UPARSE: highly accurate OTU sequences from microbial amplicon reads. *Nat Methods.* 2013;10(10):996-8.
6. Dhariwal A, Chong J, Habib S, King IL, Agellon LB, and Xia J. MicrobiomeAnalyst: a web-based tool for comprehensive statistical, visual and meta-analysis of microbiome data. *Nucleic acids research.* 2017;45(W1):W180-W8.
7. Schmid B, Tripal P, Fraass T, Kersten C, Ruder B, Gruneboom A, et al. 3Dscript: animating 3D/4D microscopy data using a natural-language-based syntax. *Nat Methods.* 2019;16(4):278-80.
8. Lotz M, Gutle D, Walther S, Menard S, Bogdan C, and Hornef MW. Postnatal acquisition of endotoxin tolerance in intestinal epithelial cells. *The Journal of experimental medicine.* 2006;203(4):973-84.
9. van der Goot AT, Zhu W, Vazquez-Manrique RP, Seinstra RI, Dettmer K, Michels H, et al. Delaying aging and the aging-associated decline in protein homeostasis by inhibition of tryptophan degradation. *Proceedings of the National Academy of Sciences of the United States of America.* 2012;109(37):14912-7.
10. Heinrikson RL, and Meredith SC. Amino acid analysis by reverse-phase high-performance liquid chromatography: precolumn derivatization with phenylisothiocyanate. *Anal Biochem.* 1984;136(1):65-74.
11. Paduch K, Debus A, Rai B, Schleicher U, and Bogdan C. Resolution of Cutaneous Leishmaniasis and Persistence of Leishmania major in the Absence of Arginase 1. *Journal of immunology.* 2019;202(5):1453-64.

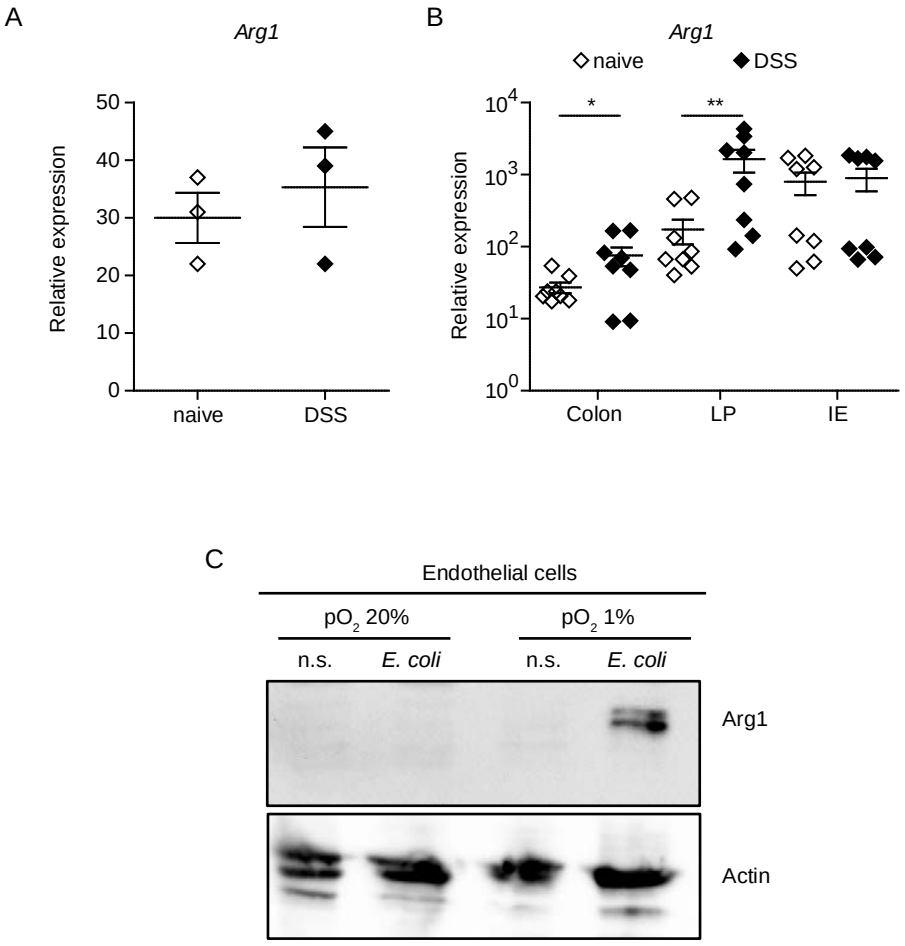

Suppl. Figure 1

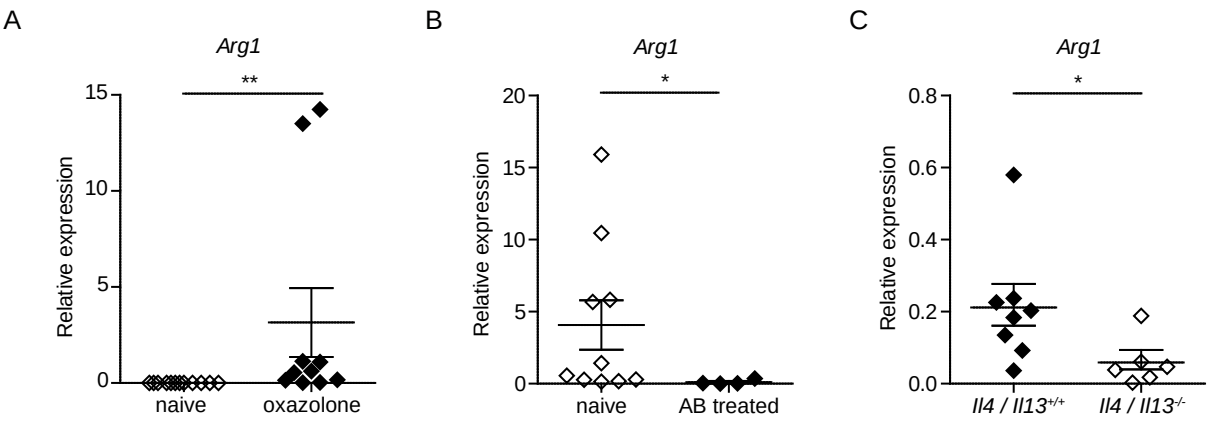

Suppl. Figure 2

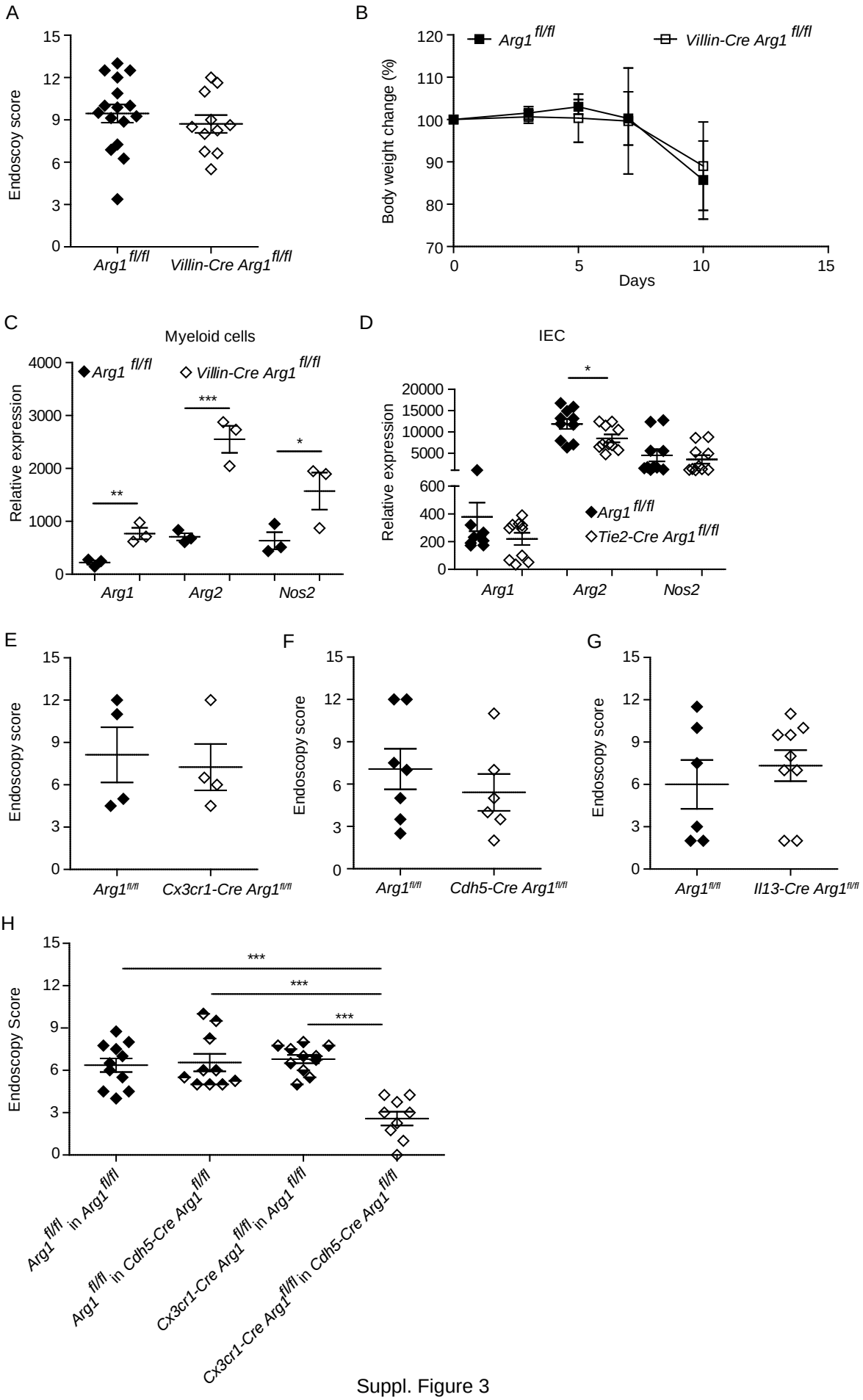

Suppl. Figure 3

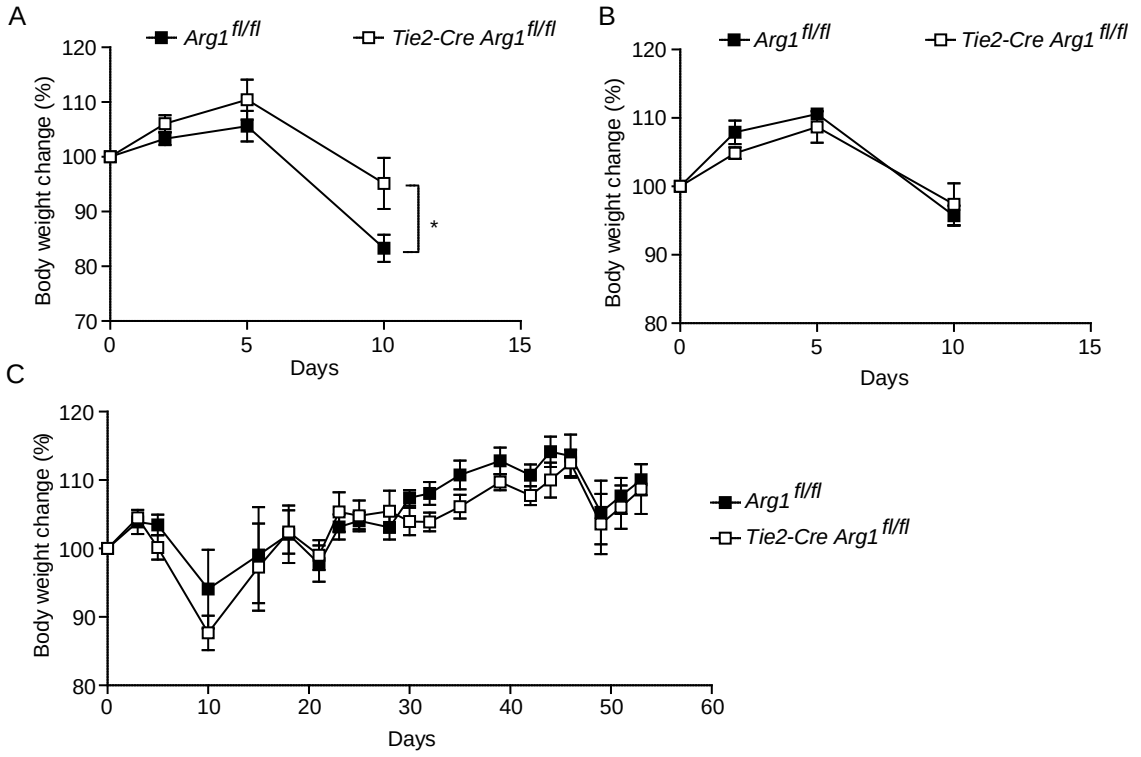

Suppl. Figure 4

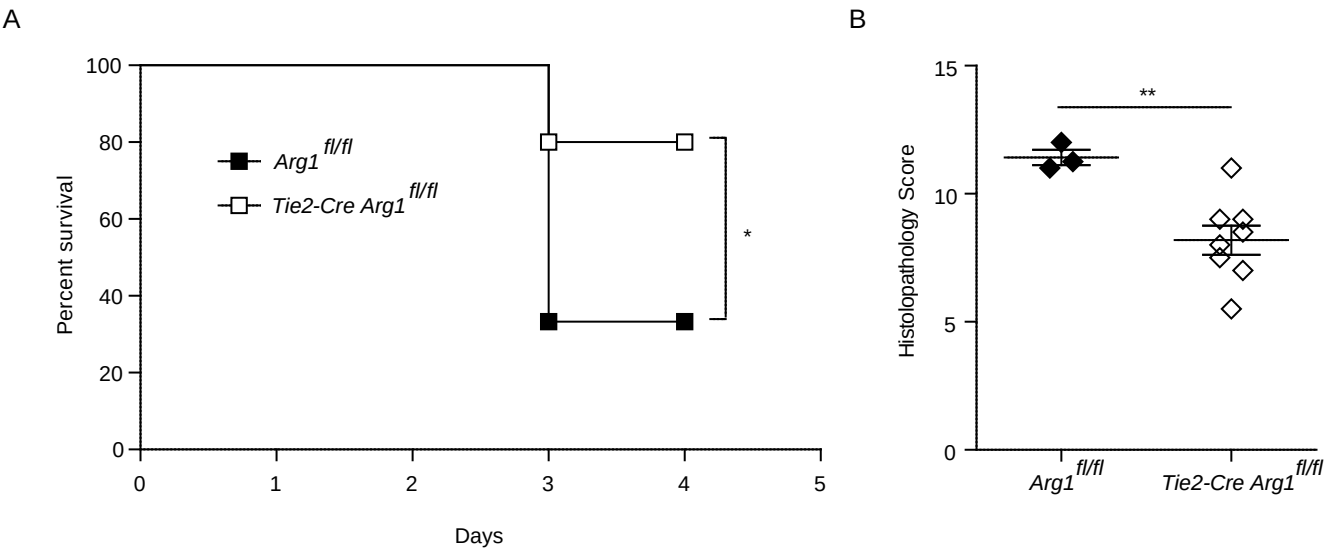

Suppl. Figure 5

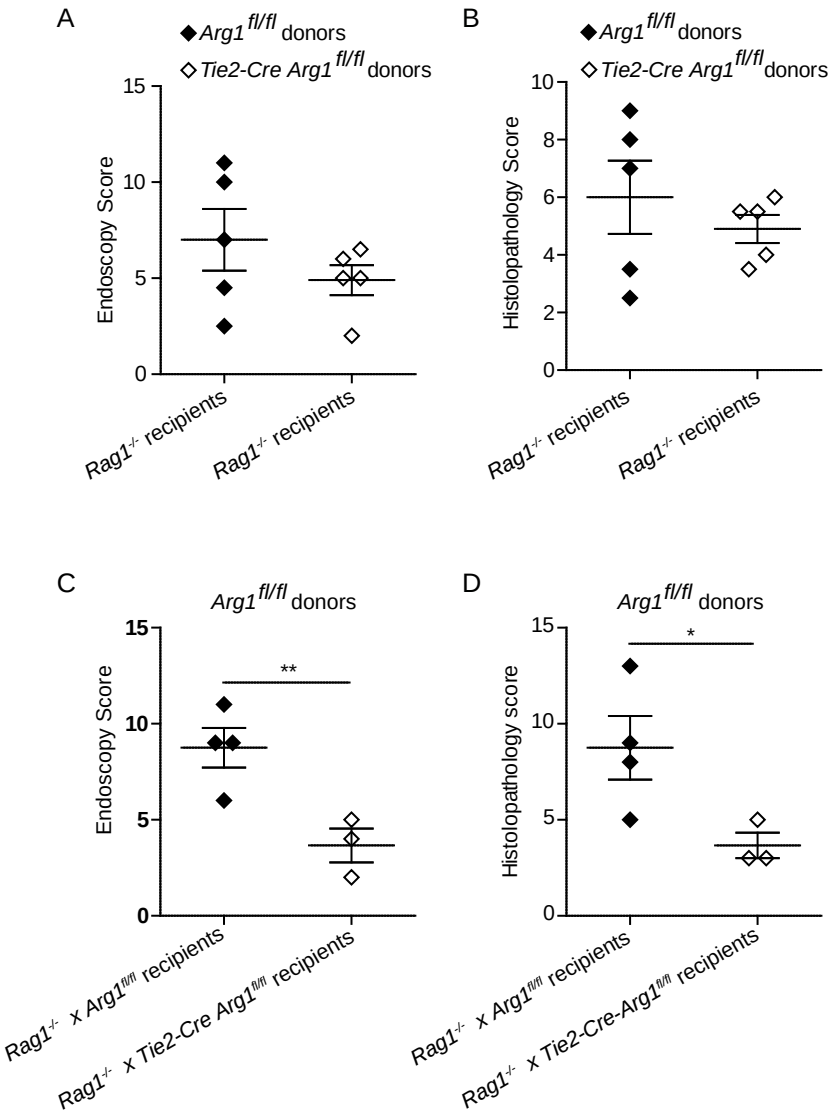

Suppl. Figure 6

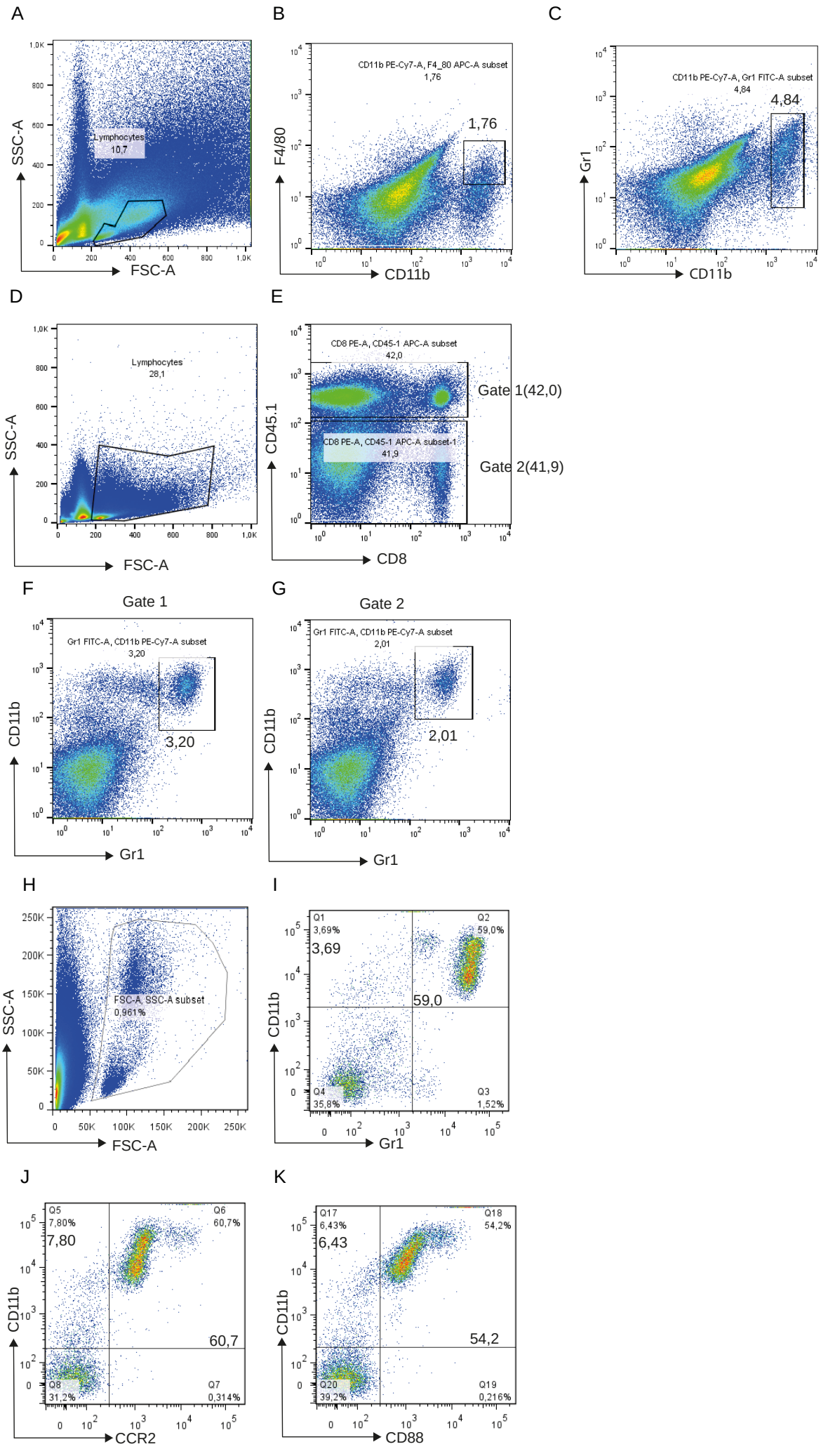

Suppl. Figure 7

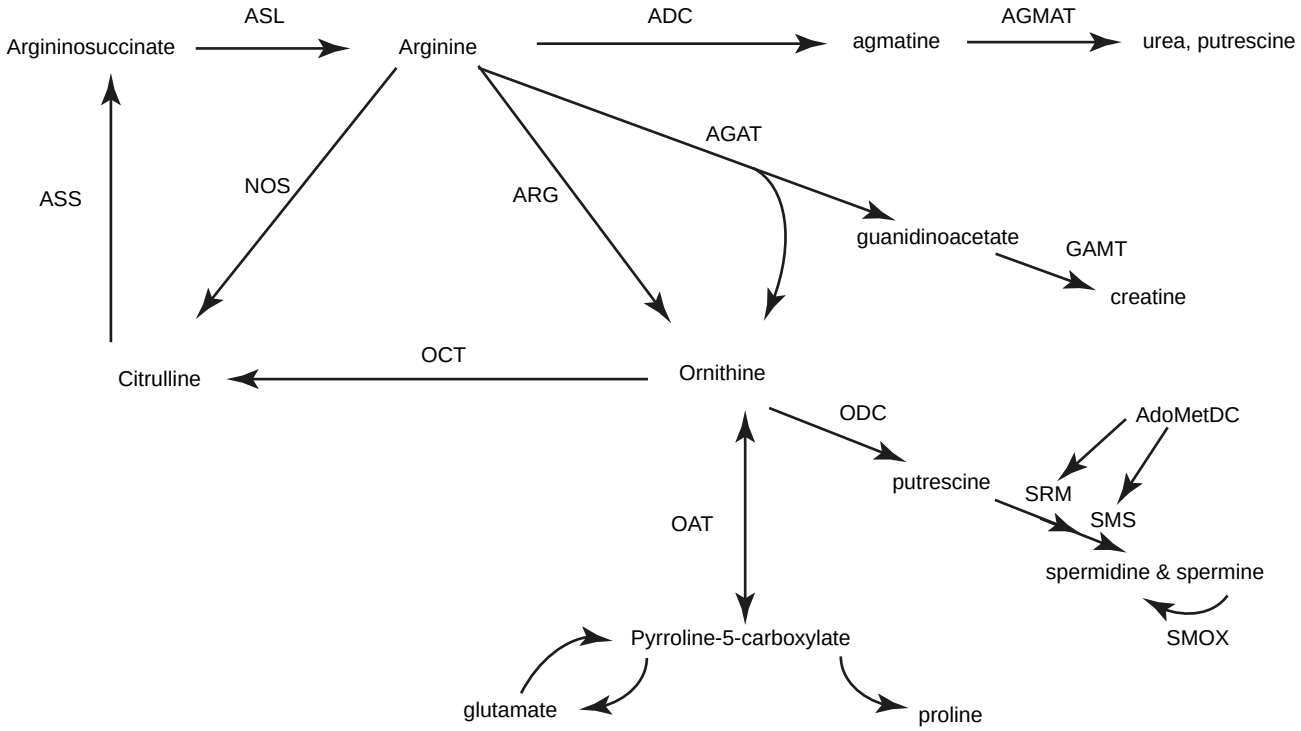

Suppl. Figure 8

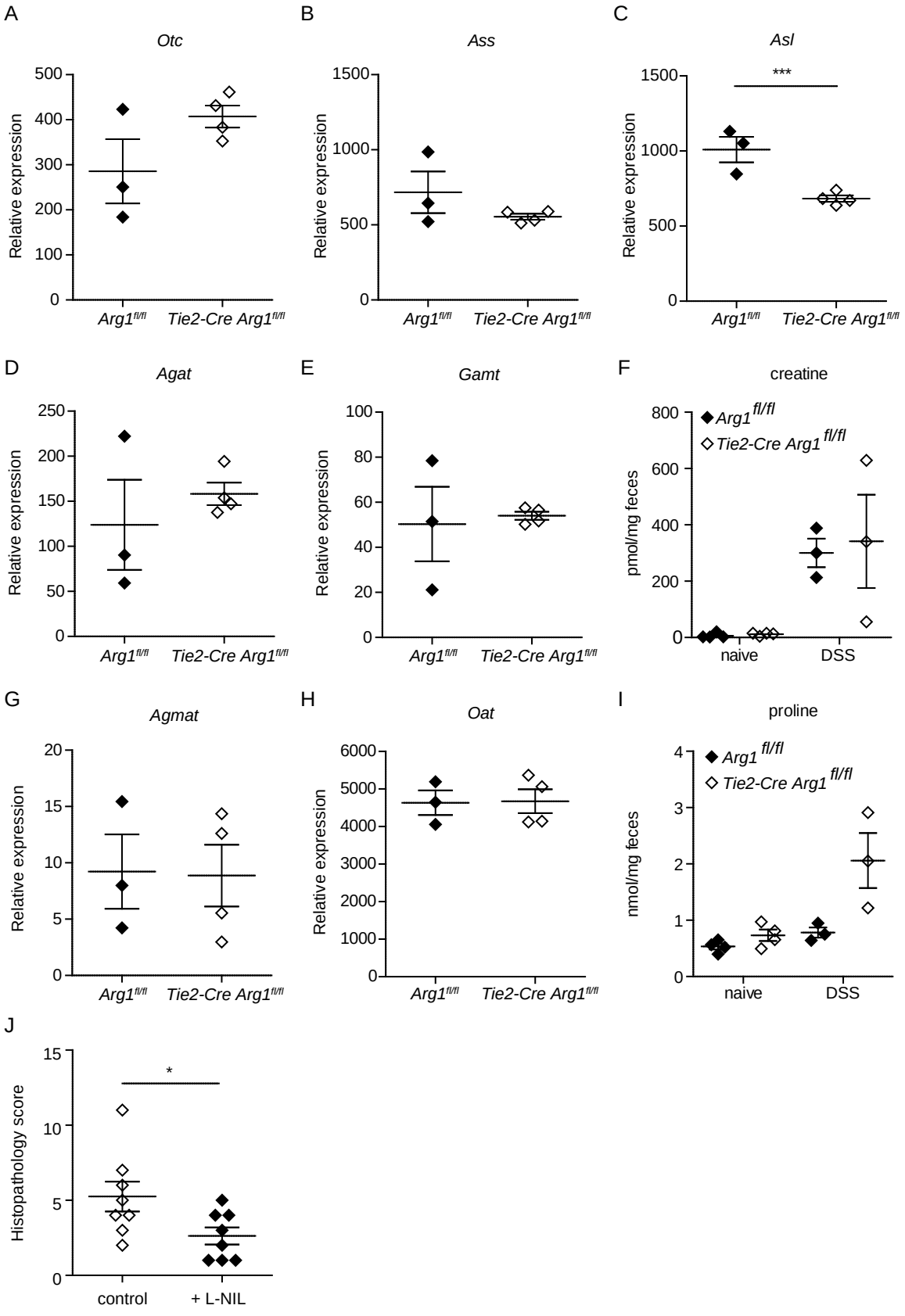

Suppl. Figure 9

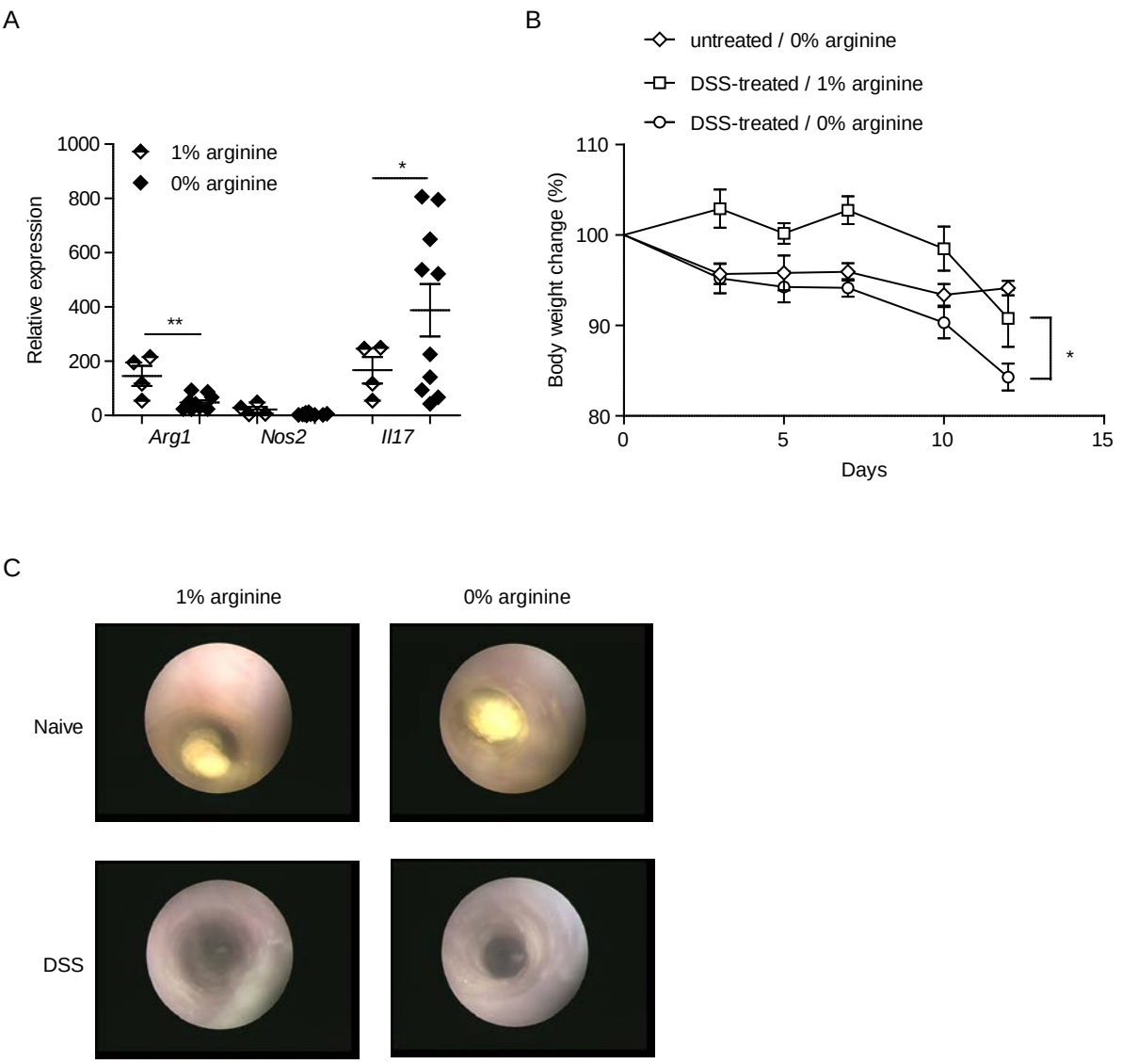

Suppl. Figure 10

A

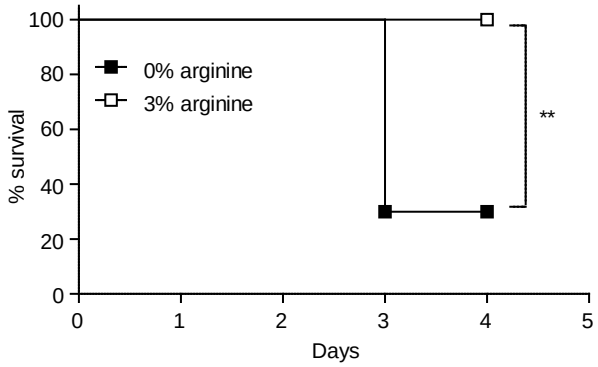

B

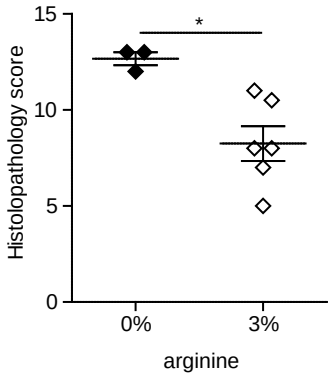

Suppl. Figure 11

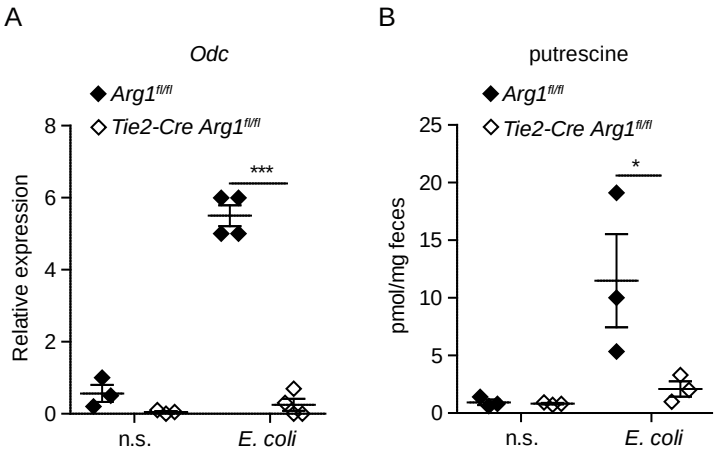

Suppl. Figure 12

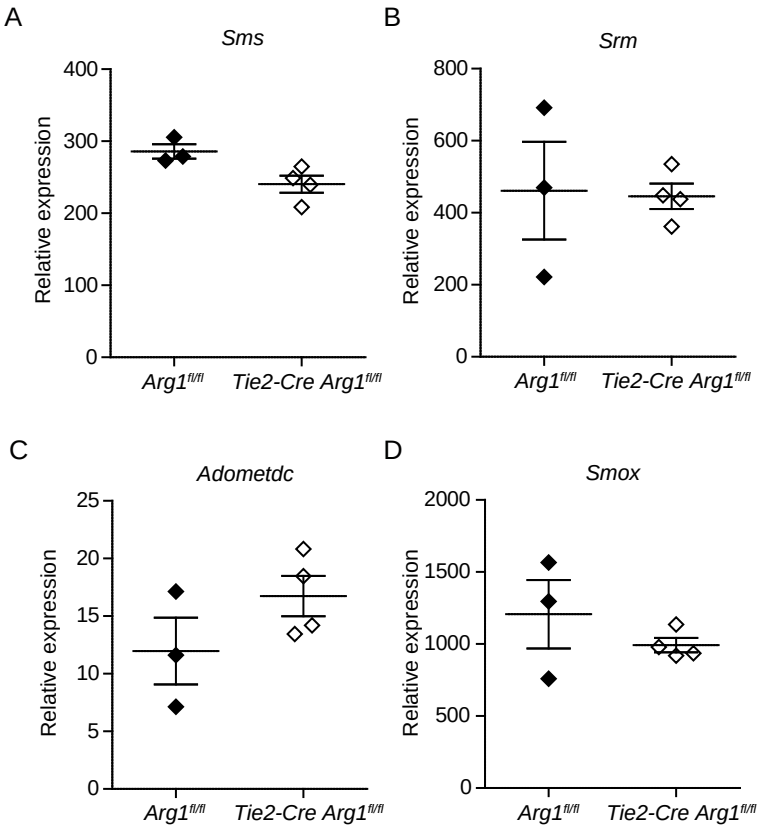

Suppl. Figure 13

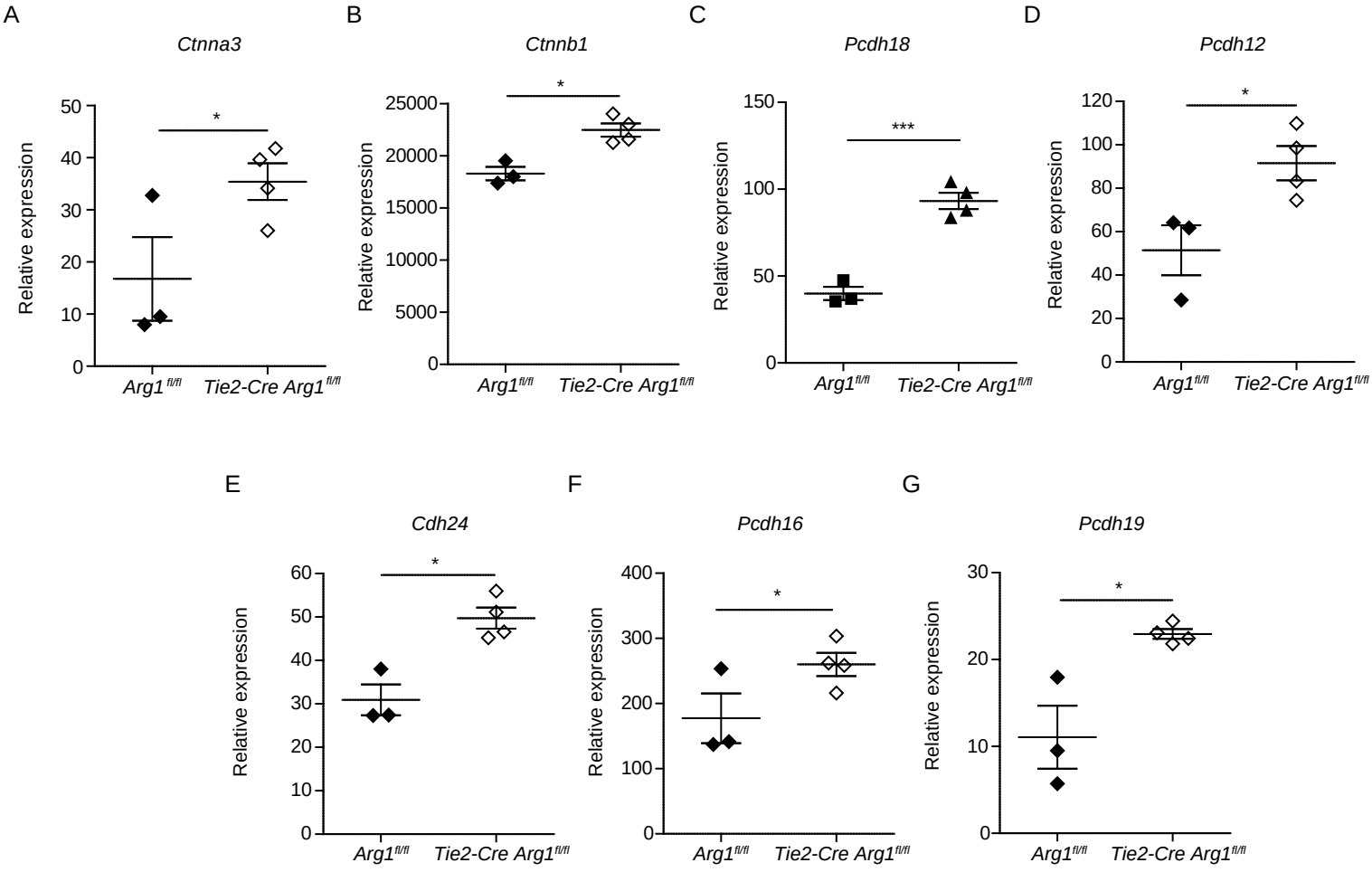

Suppl. Figure 14

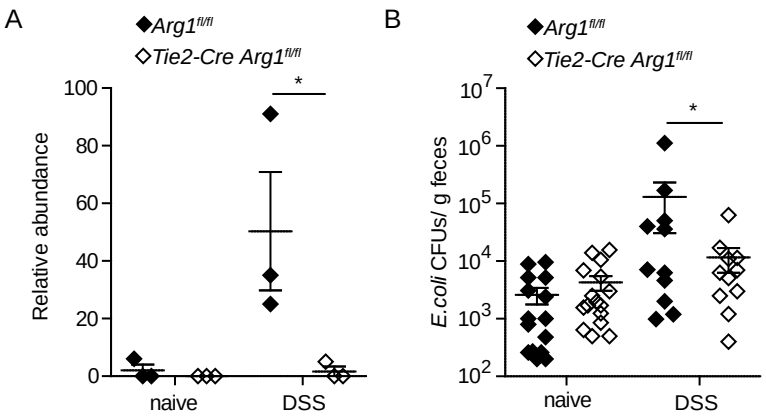

Suppl. Figure 15

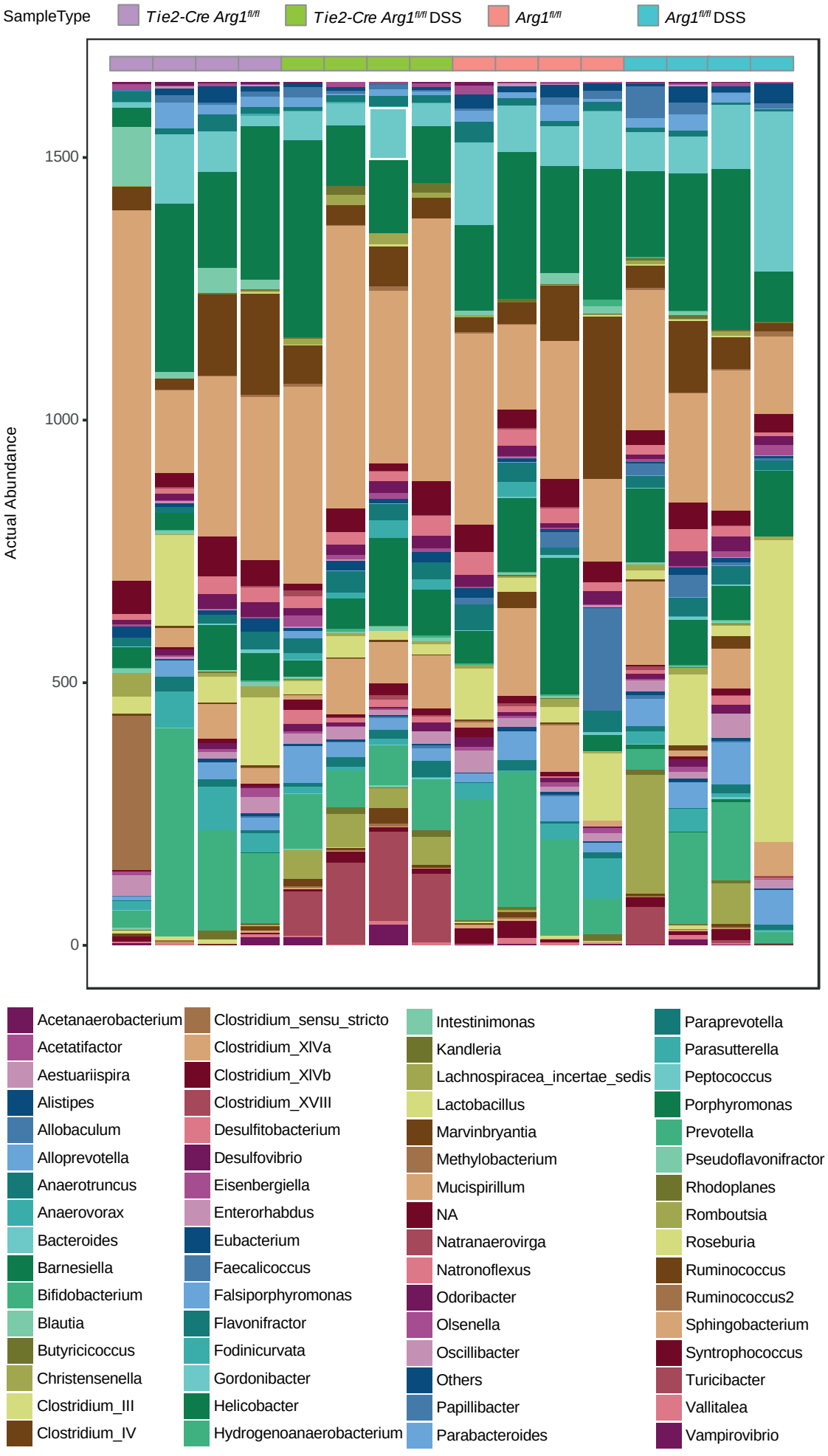

Suppl. Figure 16

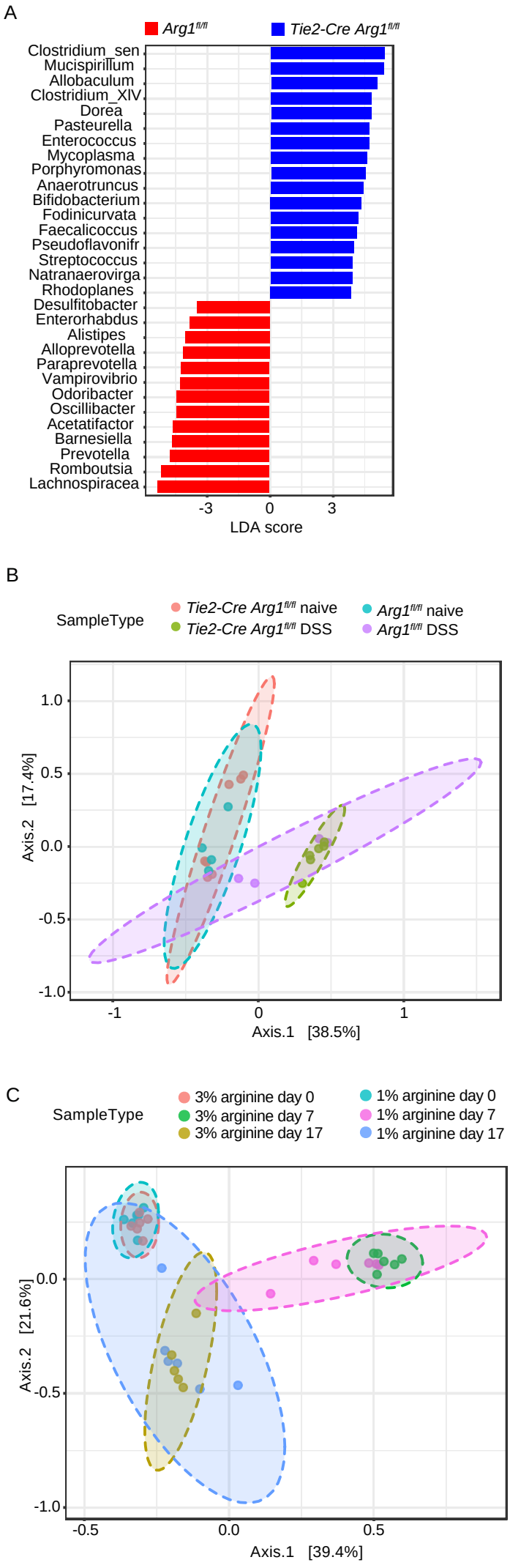

Suppl. Figure 17

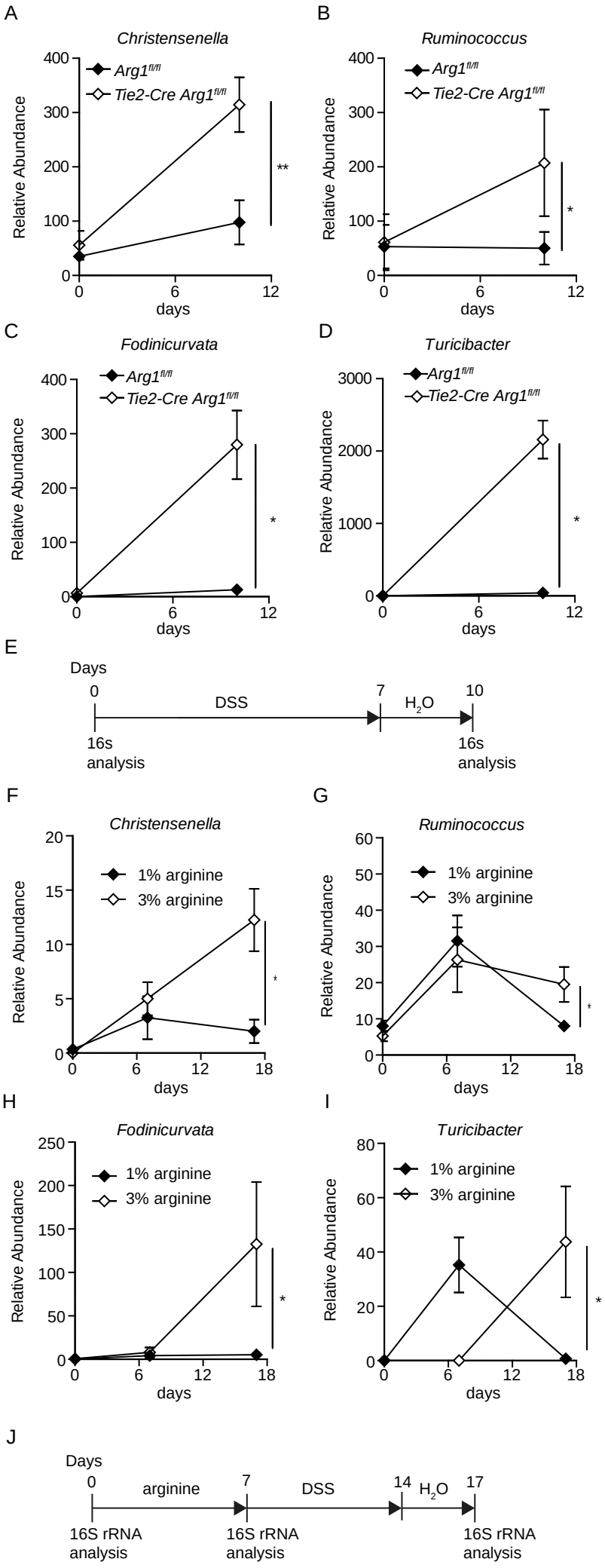

Suppl. Figure 18

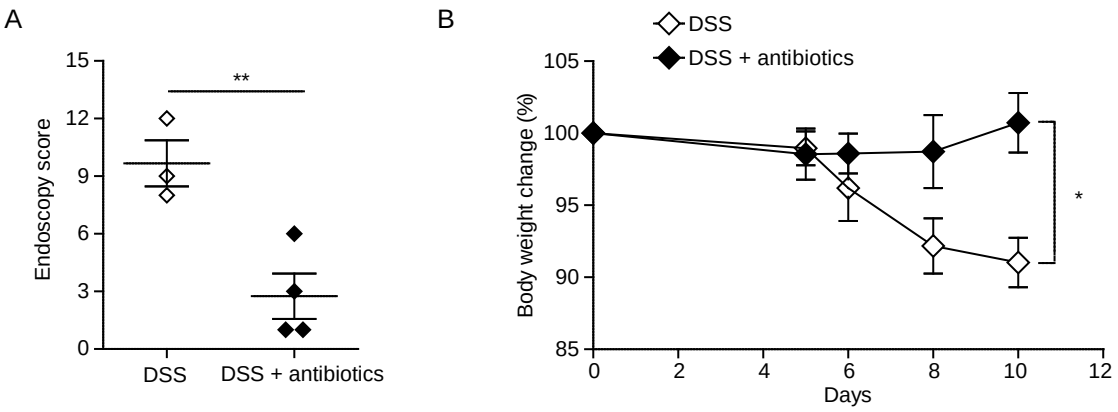

Suppl. Figure 19

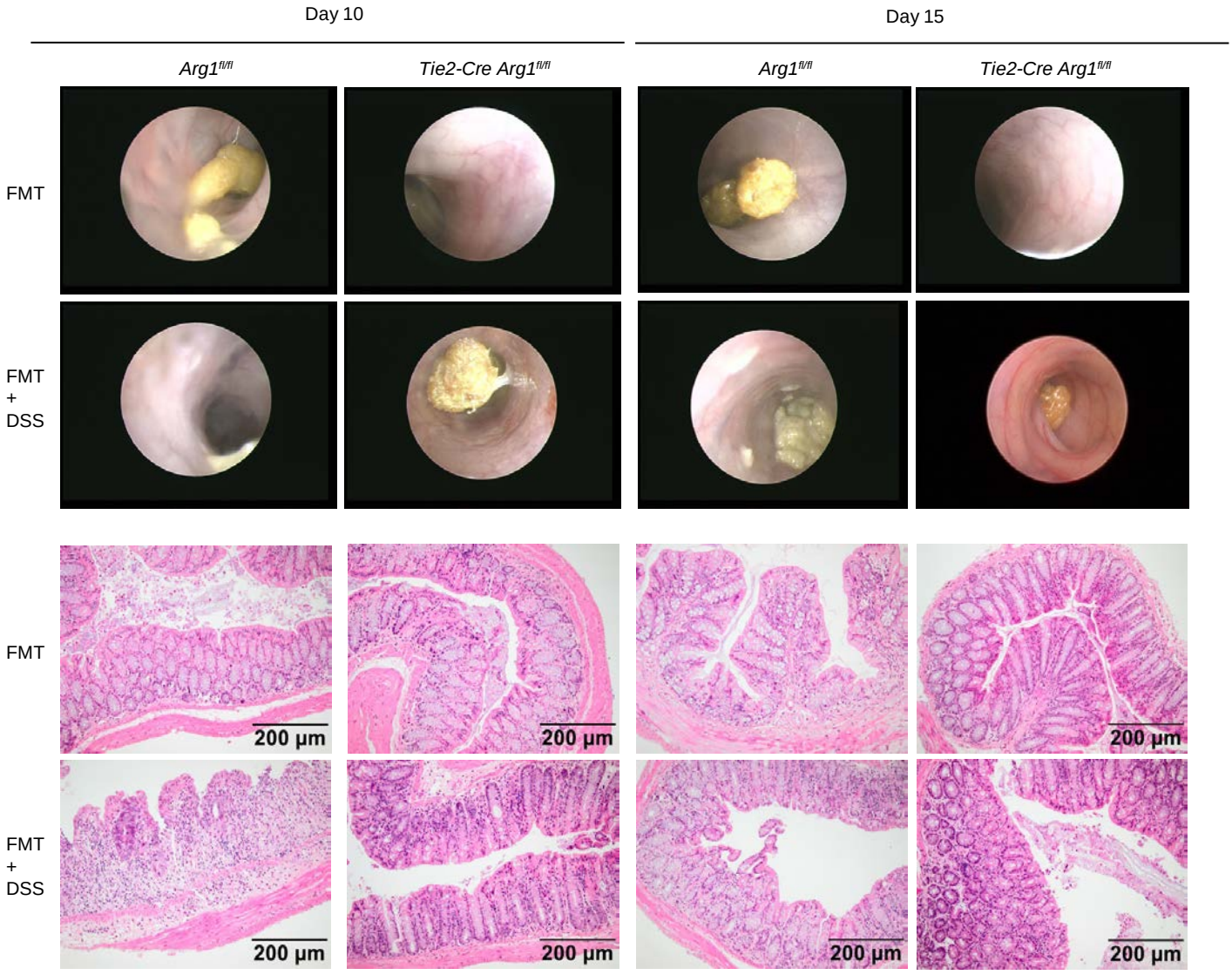

Suppl. Figure 20

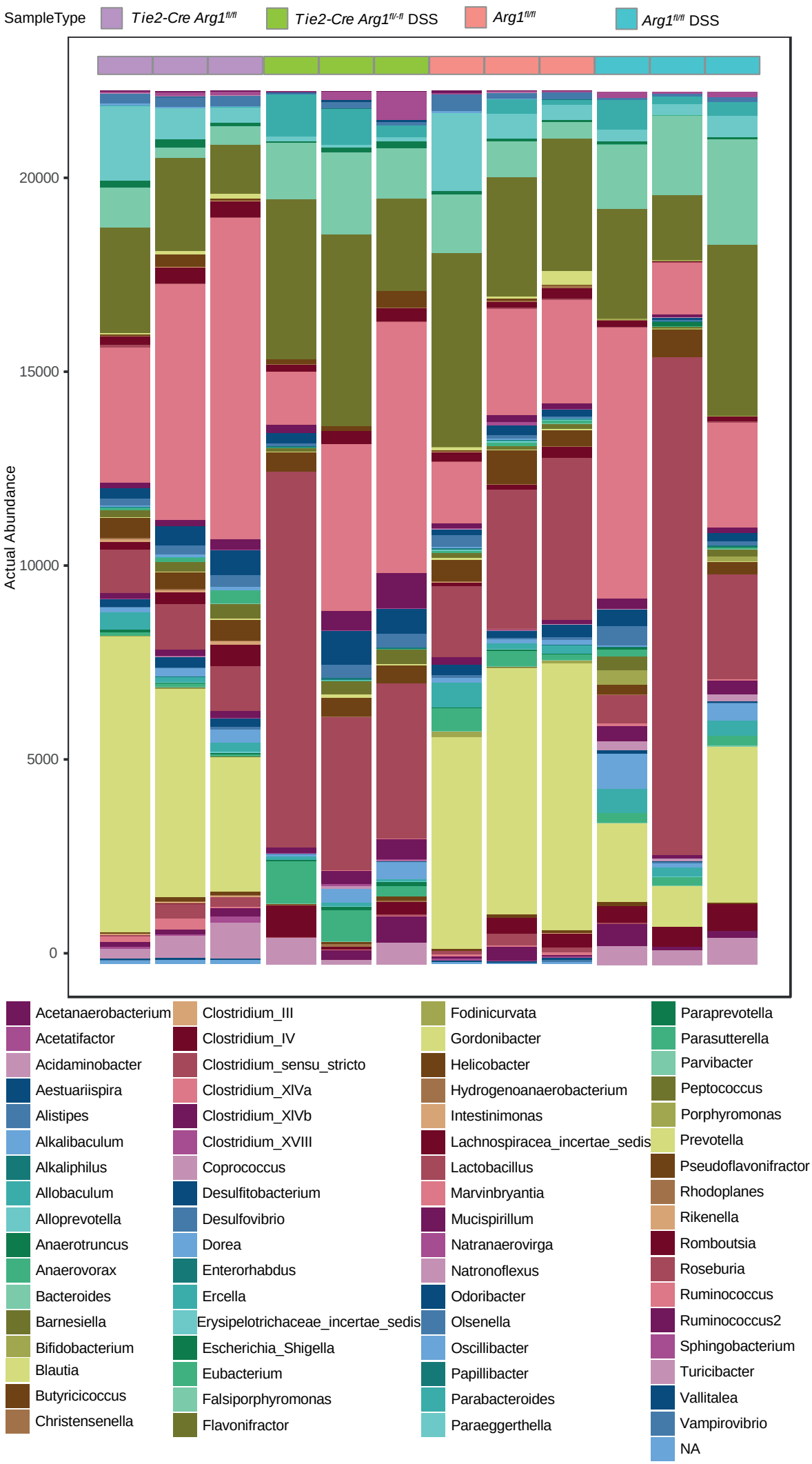

Suppl. Figure 21

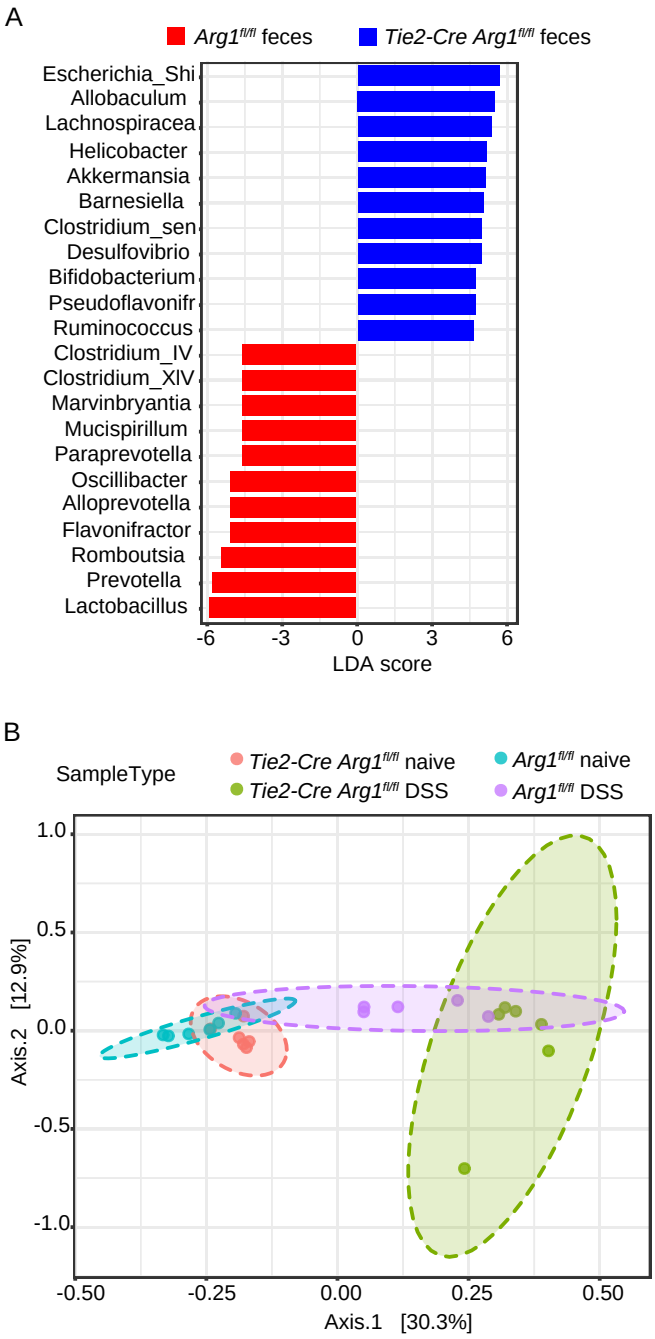

Suppl. Figure 22

A

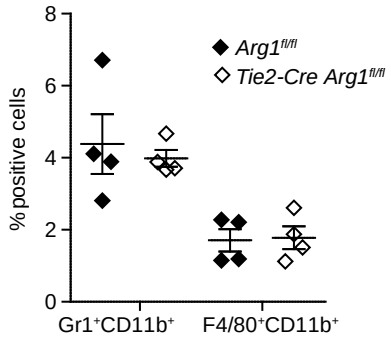

B

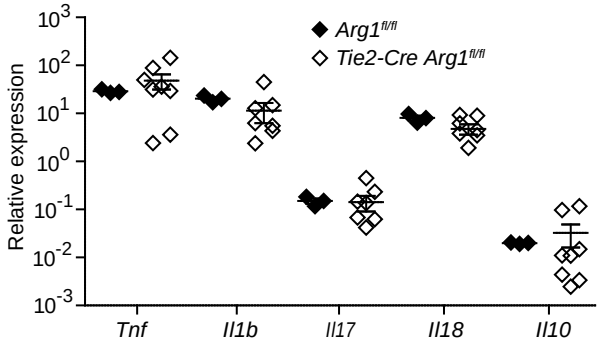

C

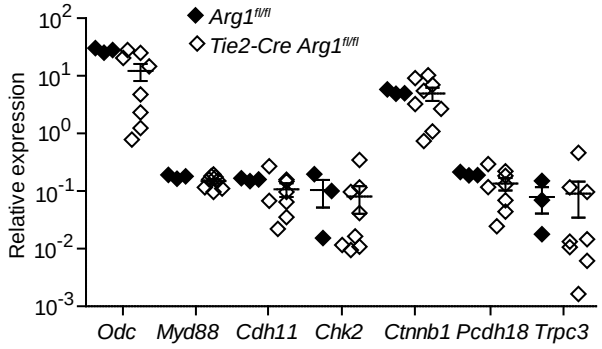

Suppl. Figure 23